Polar Spectral Scheme for the Spatially Homogeneous Boltzmann Equation

E. Fonn and P. Grohs and R. Hiptmair

Polar Spectral Scheme for the Spatially Homogeneous Boltzmann Equation

E. FONN †, P. GROHS ‡, AND R. HIPTMAIR §

Seminar for Applied Mathematics, ETH Zurich, CH-8092 Zürich

We consider the non-linear spatially homogeneous Boltzmann equation, and develop a polar spectral discretization in two dimensions based on Laguerre polynomials, which generalizes previous methods by Ender and Ender [A.YA. ENDER AND I.A. ENDER: *Polynomial expansions for the isotropic Boltzmann equation and invariance of the collision integral with respect to the choice of basis functions.* Physics of Fluids, 11:2720–2730, 1999] to the case of non-radially symmetric solutions. The method yields sparse approximation for long times and enjoys exponential convergence in the number of degrees of freedom for analytic solutions. A particular implementation exactly conserves mass, momentum and energy. Compared to the Fourier spectral discretization method, we need not truncate the collision operator and, thus, avoid aliasing errors.

Keywords: Boltzmann equartion; spectral Galerkin method; Laguerre polynomials.

1. Introduction

In this paper we are concerned with the discretization in velocity and time of the spatially homogeneous Boltzmann equation

$$\frac{\partial f}{\partial t}(t,\boldsymbol{v}) = Q(f,f)(t,\boldsymbol{v}), \tag{1.1}$$

where $f : \mathbb{R}^+ \times \mathbb{R}^d \to \mathbb{R}^+$ is an unknown density function, for which initial values $f_0 = f_0(\boldsymbol{v})$ at $t = 0$ are prescribed. The bilinear collision operator Q takes the form (dropping the variable t for the sake of readability)

$$Q(f,h)(\boldsymbol{v}) = \int_{\mathbb{R}^d} \int_{S^{d-1}} B(\|\boldsymbol{v}-\boldsymbol{v}_*\|, \cos\theta)(h'_* f' - h_* f) \, \mathrm{d}\boldsymbol{\sigma} \, \mathrm{d}\boldsymbol{v}_*, \tag{1.2}$$

where the notation $Q(f,h)(\boldsymbol{v})$ means $Q(f,h)$ evaluated at $\boldsymbol{v}$, and we have used the common shorthand notation

$$f = f(\boldsymbol{v}), \qquad h_* = h(\boldsymbol{v}_*), \qquad f' = f(\boldsymbol{v}'), \qquad h'_* = h(\boldsymbol{v}'_*).$$

The pre- and post-collision velocities $(\boldsymbol{v}, \boldsymbol{v}_*)$ and $(\boldsymbol{v}', \boldsymbol{v}'_*)$ are related through the transformation

$$\boldsymbol{v}' = \frac{1}{2}(\boldsymbol{v}+\boldsymbol{v}_* + \|\boldsymbol{v}-\boldsymbol{v}_*\|\boldsymbol{\sigma}), \qquad \boldsymbol{v}'_* = \frac{1}{2}(\boldsymbol{v}+\boldsymbol{v}_* - \|\boldsymbol{v}-\boldsymbol{v}_*\|\boldsymbol{\sigma}),$$

which represents all solutions conserving momentum and energy, parametrized by $\boldsymbol{\sigma} \in S^{d-1}$. See Figure 1.
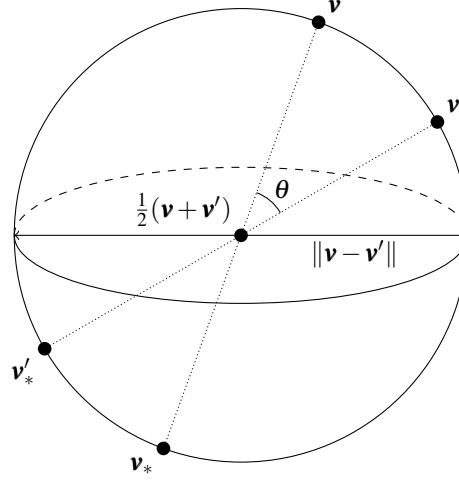

FIG. 1: Illustrating the relationship between pre- and post-collisional velocities. On a sphere centered at $1/2\,(\boldsymbol{v}+\boldsymbol{v}_*)$ with diameter $\|\boldsymbol{v}-\boldsymbol{v}_*\|$, the pre-collisional velocities are diametrically opposite, as are the post-collisional velocities. The angle between the two is the θ entering (1.2).

By construction Q enjoys invariance with respect to translations and rotations, as expressed in the following theorem. Actually, these properties are

THEOREM 1.1 For $\boldsymbol{c} \in \mathbb{R}^d$, let $\tau_{\boldsymbol{c}}$ be a translation operator, i.e. $\tau_{\boldsymbol{c}} f(\boldsymbol{x}) = f(\boldsymbol{x}-\boldsymbol{c})$. Also, given a rotation matrix $R \in \mathbb{R}^{d \times d}$, let ρ_R be a rotation operator, i.e. $\rho_R f(\boldsymbol{x}) = f(R\boldsymbol{x})$. Then Q commutes with $\tau_{\boldsymbol{c}}$ and ρ_R:

$$Q(\tau_{\boldsymbol{c}} f, \tau_{\boldsymbol{c}} g) = \tau_{\boldsymbol{c}} Q(f,g), \qquad Q(\rho_R f, \rho_R g) = \rho_R Q(f,g).$$

The two terms $h'_* f'$ and $h_* f$ are called *gain* and *loss* parts respectively, and it is often useful (and we will do so when necessary) to split the collision operator and write

$$Q(f,h) = Q^+(f,h) - Q^-(f,h). \tag{1.3}$$

We are going to use this splitting in our spectral method. This is only possible, if we make the following customary assumption on the collision kernel B in (1.2).

Assumption 1.2 Assume that B is separable, with a power law dependence on the relative velocity, that is,

$$B(\|\boldsymbol{u}\|, \cos\theta) = \|\boldsymbol{u}\|^\lambda b(\cos\theta), \qquad \text{with} \quad \lambda \geqslant -\frac{d}{2}, \tag{1.4}$$

and some function $b : [-1,1] \to \mathbb{R}$ that satisfies *Grad's cutoff assumption*

$$\int_{S^{d-1}} b(\cos\theta)\,\mathrm{d}\boldsymbol{\sigma} < \infty. \tag{1.5}$$

For the physical background and the mathematical analysis of (1.1) we refer to Cercignani (2002); Villani (2002). The numerical treatment of (1.1) has received considerable attention as a testbed for the

discretization of the full Boltzmann equation in velocity space. Among others, we would like to mention Gamba & Tharkabhushanam (2009); more references are given below.

The most popular methods for the solution of (1.1) are stochastic Monte Carlo-type methods as developed in Rjasanow & Wagner (2005). These are commonly afflicted by indeterminism, noise and slow convergence. In principle, deterministic schemes can overcome these problems, but they often incur hefty computational cost. Lattice Boltzmann methods, which rely on very crude pointwise discretizations in velocity space, have also become popular. Since our work is primarily concerned with a high-accuracy spectral deterministic method, no attempt will be made in the following to compare our work with stochastic methods or lattice Boltzmann methods.

Most existing work tackle the discretization of (1.1) by means of Fourier spectral methods. They can exploit the convolution structure of Q, which follows from Theorem 1.1. This is explained in Bobylev (1988); Kirsch & Rjasanow (2007); Pareschi & Perthame (1996) and we refer to Gamba & Tharkabhushanam (2009, 2010); Filbet *et al.* (2006); Pareschi & Russo (2000); Pareschi *et al.* (2003) for numerical simulations based on that method, and Filbet & Mouhot (2011); Fonn *et al.* (2012) for its numerical analysis. We remark that the difference methods developed in Bobylev & Rjasanow (1997, 1999, 2000) and Ibragimov & Rjasanow (2002) are related to Fourier spectral discretization.

Yet, the Fourier spectral approach entails tinkering with the collision operator in two ways:

(i) the restriction of the integration over $\mathbb{R}^d$ in (1.2) to a ball of finite radius $R > 0$.

(ii) the truncation of the velocity space $\mathbb{R}^d$ to a cube $\mathscr{D}_L := [-L,L]^d$ plus periodic continuation.

These modifications result in a perturbed evolution

$$\frac{\partial}{\partial t} f_R = Q^R(f_R, f_R), \qquad f_R(0) = f_0. \tag{1.6}$$

The evolution (1.6) is then projected onto a subset of $L^2(\mathscr{D}_L)$ spanned by a finite set of tensor product Fourier modes. One observes the following property of Q^R, which follows from the translation invariance of Q:

$$Q^R(\mathrm{e}^{\mathrm{i}\boldsymbol{l}\cdot\boldsymbol{v}}, \mathrm{e}^{\mathrm{i}\boldsymbol{m}\cdot\boldsymbol{v}}) = \hat{\beta}(\boldsymbol{l},\boldsymbol{m})\mathrm{e}^{\mathrm{i}(\boldsymbol{l}+\boldsymbol{m})\cdot\boldsymbol{v}}, \tag{1.7}$$

where $\hat{\beta}(\boldsymbol{l},\boldsymbol{m}) \in \mathbb{C}$. In other words, the collision operator is sparse with respect to this basis. With N degrees of freedom in each direction, a discrete collision operator can be applied in $\mathscr{O}(N^{2d})$ time instead of $\mathscr{O}(N^{3d})$. For some collision kernels B, this may be further improved upon, see Mouhot & Pareschi (2006) for some examples.

The price we pay for this property is a lack of conservation (the projected equation (1.6) cannot in general conserve momentum and energy), and an additional error introduced by truncation. To curb this error, the quantity R must be chosen large enough compared to the effective support of f, and the ratio $R : L$ must be chosen small enough to avoid aliasing between different periodizations of f Fonn *et al.* (2012). However, increasing L will effectively increase the high-frequency content of f, so the trial space must be enlarged as well.

In this paper, we propose a different discrete trial space for f, which avoids the shortcomings of the Fourier spectral method. To begin with, the proposed method is fully conservative (in mass, momentum and energy) for a certain choice of parameters. It also requires no truncation of the collision operator, so no aliasing occurs. The price we pay for these properties is a worse time complexity (in two dimensions, it requires $\mathscr{O}(N^5)$ time to apply the collision operator, compared to the Fourier method's $\mathscr{O}(N^4)$), but this is mitigated in part by a natural sparsity for long times, which can be exploited by a time-dependent adaptive choice of the trial space.

Associated Laguerre polynomials (also called *generalized* Laguerre polynomials or *Sonine* polynomials have been used before to solve the Boltzmann equation (in particular, see work by Ender and Ender Ender & Ender (1994, 1999), the former appears unavailable in English), but only for rotationally symmetric solutions. In this paper we generalized the system to arbitrary solutions in two dimensions. We study the approximation properties of the trial space in Section 2 and prove exponential convergence of the best approximation in terms of the number of degrees of freedom for analytic densities. Yet, so far there is no proof that this kind of convergence carries over to the solution of the semi-discrete evolution. Some algorithmic details of the polar spectral method are given in Section 4.1, whereas Section 5 reports its performance in the case of a few test problems. Our results provide circumstantial evidence that The full generalization of the method to arbitrary dimensions is postponed to future work; for the remainder of the paper, we focus on two-dimensional velocity space.

Parallel to our work a closely related Petrov-Galerkin spectral scheme for (1.1) has been developed by Kitzler & Schöberl (2013). They use Maxwellian modulated tensor product polynomials as trial space and test with the same polynomials, which ensures conservation of mass, momentum and energy for the semi-discrete evolution. In their work, for the simple case of Maxwellian molecules $B \equiv 1$, they rely on a transformation to a polar spectral representation to accelerate the application of the collision operator in their discrete framework. In addition, a quadrature approximation is employed. Though not explicitly stated in Kitzler & Schöberl (2013), taking into account that the accuracy of the quadrature has to match the resolution of the trial space, we end up with asymptotic computational costs of $\mathcal{O}(N^5)$ per timestep, the same as for the method presented in this article. A thorough comparison of the methods still has to be done.

2. The polar Laguerre function space

For the sake of simplicity of notation we will identify $\mathbb{R}^2$ with $\mathbb{C}$, and its standard polar representation,

$$\boldsymbol{v} = x(\boldsymbol{v}) + \mathrm{i}y(\boldsymbol{v}) = r(\boldsymbol{v})\mathrm{e}^{\mathrm{i}\arg\boldsymbol{v}}.$$

We will also denote by μ the Maxwellian weight function

$$\mu(\boldsymbol{v}) = \mu(r) = \mathrm{e}^{-r^2}. \tag{2.1}$$

Let us now define, for $l \in \mathbb{Z}, k \in \mathbb{Z}_{\geqslant 0}, \beta > 0$

$$\xi_l : \quad [0, 2\pi) \to \mathbb{C} \quad : \quad \theta \mapsto \mathrm{e}^{\mathrm{i}l\theta}, \tag{2.2}$$

$$\psi_{k,\beta}^{\mathrm{S}} : \quad [0, \infty) \to \mathbb{R} \quad : \quad r \mapsto \sqrt{2}\mathrm{e}^{-r^2/\beta}L_k^{(0)}(r^2), \tag{2.3}$$

$$\psi_{k,\beta}^{\mathrm{K}} : \quad [0, \infty) \to \mathbb{R} \quad : \quad r \mapsto \sqrt{\frac{2}{k+1}}\mathrm{e}^{-r^2/\beta}rL_k^{(1)}(r^2). \tag{2.4}$$

Here, $L_k^{(\alpha)}$ denote the associated Laguerre polynomials of order $\alpha \in \mathbb{N}_0$. They are defined as

$$L_k^{(\alpha)}(x) = \sum_{i=0}^{k}(-1)^k\binom{k+\alpha}{k-i}\frac{x^i}{i!}, \tag{2.5}$$

k	$L_k^{(0)}$	$L_k^{(1)}$
0	1	1
1	$-x+1$	$-x+2$
2	$\frac{1}{2}x^2 - 2x + 1$	$\frac{1}{2}x^2 - 3x + 3$
3	$-\frac{1}{6}x^3 + \frac{3}{2}x^2 - 3x + 1$	$-\frac{1}{6}x^3 + 2x^2 - 6x + 4$
4	$\frac{1}{24}x^4 - \frac{2}{3}x^3 + 3x^2 - 4x + 1$	$\frac{1}{24}x^4 - \frac{5}{6}x^3 + 5x^2 - 10x + 5$

Table 1: The first few associated Laguerre polynomials of order 0 and 1.

and satisfy the recurrence relations

$$(k+1)L_{k+1}^{(0)}(x) = (2k+1-x)L_k^{(0)}(x) - kL_{k-1}^{(0)}(x), \qquad k \geqslant 1, \tag{2.6}$$

$$L_k^{(\alpha)}(x) = \sum_{i=0}^{k} L_i^{(\alpha-1)}(x), \tag{2.7}$$

with $L_0^{(0)} = 1$ and $L_1^{(0)} = 1 - x$. The first few polynomials of order 0 and 1 are tabulated in Table 1 and plotted in Figure 2.
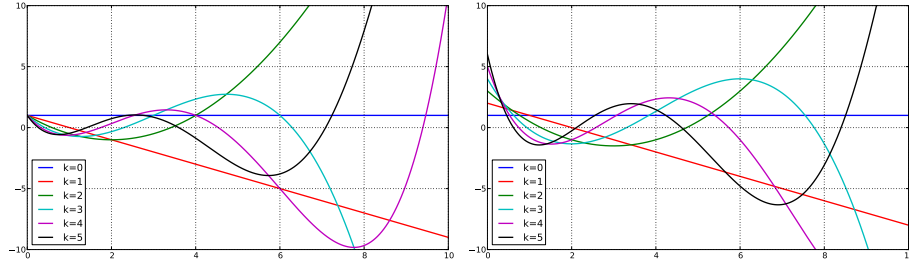

FIG. 2: The first six associated Laguerre polynomials of order 0 (left) and 1 (right).

The polynomials $L_k^{(\alpha)}$ are orthogonal with respect to the weight $e^{-x}x^{\alpha}$:

$$\int_0^{\infty} e^{-x}x^{\alpha} L_k^{(\alpha)}(x) L_l^{(\alpha)}(x)\,dx = \binom{k+\alpha}{k}\alpha! \tag{2.8}$$

This is the motivation for the definitions (2.3) and (2.4). Substituting $x = r^2$, we see that $\psi_{k,\beta}^S$ and $\psi_{k,\beta}^K$ are orthonormal with respect to the weighted L^2 inner product on $(0, \infty)$ with weight

$$e^{-(1-2/\beta)r^2} r\,dr,$$

which fits with the volume element for polar integrals over $\mathbb{R}^2$. This will be made precise in the following.

The functions ψ_k^S and ψ_k^K from (2.3), (2.4) are exponentially weighted polynomials in r of degree $2k$ and $2k+1$ containing only even and odd powers of r, respectively. Therefore it can be expected that, if $f : [0, \infty) \to \mathbb{R}$ is analytic and sufficiently rapidly decaying (a condition depending on β) and its analytic extension to $\mathbb{R}$ is even, it will have an exponentially convergent series representation in terms of the functions $\psi_{k,\beta}^S$, and likewise for $\psi_{k,\beta}^K$ if f has an odd extension to $\mathbb{R}$. The appropriate domains of analyticity turn out to be strips

$$s(c) := \{z \,:\, |\Im z| \leqslant \sqrt{c}\} \tag{2.9}$$

PROPOSITION 2.1 Let $f : [0, \infty) \to \mathbb{R}$ be given, and assume that f has an even analytic extension to the strip $s(c)$ for some $c > 0$, and that for every b such that $0 \leqslant b < c$, there exists $C(b)$ such that

$$|f(z)| \leqslant C(b) \exp\left[\frac{x^2}{2} - |y|\left(b^2 - y^2\right)^{\frac{1}{2}}\right], \tag{2.10}$$

for all $z = x + iy \in s(b)$. Then there exist Laguerre series expansions, converging to f uniformly on compact sets,

$$f(r) = \sum_{k=0}^{\infty} a_k^{(0)} L_k^{(0)}(r^2) = \sum_{k=0}^{\infty} a_k^{(1)} L_k^{(1)}(r^2),$$

where the coefficients $a_k^{(\alpha)}$ for $\alpha \in \{0, 1\}$ are given by

$$a_k^{(\alpha)} = \frac{1}{(k+1)^{\alpha/2}} \int_0^{\infty} e^{-x} x^{\alpha} L_k^{(\alpha)}(x) f(\sqrt{x})\, dx$$

and satisfy the decay property

$$\left|a_k^{(\alpha)}\right| \leqslant 2C(b) e^{-2b\sqrt{k}}. \tag{2.11}$$

Proof. The existence of a Laguerre series expansion of f is confirmed by (Szsz & Yeardley, 1958, Theorem B). By (Szsz & Yeardley, 1958, Lemma 3.4) we also conclude (2.11) for $\alpha = 0$ and all b.

The corresponding decay for $a_k^{(1)}$ holds due to the relation $a_k^{(1)} = a_k^{(0)} - a_{k+1}^{(0)}$, which follows easily from the next lemma. $\qquad\square$

LEMMA 2.1 The Laguerre polynomials satisfy

$$xL_k^{(1)}(x) = (k+1)(L_k^{(0)}(x) - L_{k+1}^{(0)}(x)).$$

Proof. We proceed by induction. As $L_0^{(0)}(x) = 1$ and $L_1^{(0)}(x) = 1 - x$, the statement is evidently true for $k = 0$. For the induction step, we note that

$$\begin{aligned}
xL_k^{(1)} &\overset{(2.7)}{=} xL_{k-1}^{(1)} + xL_k^{(0)} \\
&\overset{\text{IH}}{=} k(L_{k-1}^{(0)} - L_k^{(0)}) + xL_k^{(0)} \\
&\overset{(2.6)}{=} k(L_{k-1}^{(0)} - L_k^{(0)}) + (2k+1)L_k^{(0)} - kL_{k+1}^{(0)} - (k+1)L_{k+1}^{(0)} \\
&= (k+1)(L_k^{(0)} - L_{k+1}^{(0)}),
\end{aligned}$$

where the induction hypothesis was used in step (IH). $\qquad\square$

Proposition 2.1 establishes sufficient conditions on a function f to have a rapidly converging Laguerre series expansion comprising terms $L_k^{(\alpha)}(r^2)$ for $\alpha \in \{0, 1\}$. Now, we consider expansions of even and odd functions in terms of ψ^S and ψ^K.

PROPOSITION 2.2 Let $f^S, f^K : [0, \infty) \to \mathbb{R}$ be given. Assume that f^S and $\frac{1}{r} f^K$ have analytic even and odd extensions, respectively, to the strip $s(c)$ for some $c > 0$, and that for every b such that $0 \leqslant b < c$, there exists $C(b)$ such that

$$|f^S(z)|, \left| \frac{1}{z} f^K(z) \right| \leqslant C(b) \exp \left[-\frac{|z|^2}{\beta} + \frac{x^2}{2} - |y| \left(b^2 - y^2 \right)^{\frac{1}{2}} \right], \tag{2.12}$$

for all $z = x + iy \in s(b)$. Then there exist series representations

$$f^S(r) = \sum_{k=0}^{\infty} a_{k,\beta}^S \psi_{k,\beta}^S(r), \qquad f^K(r) = \sum_{k=0}^{\infty} a_{k,\beta}^K \psi_{k,\beta}^K(r), \tag{2.13}$$

that converge uniformly on each compact interval. Using the Maxwellian weight μ as defined in (2.1), the expansion coefficients are given by

$$
\begin{aligned}
a_{k,\beta}^S &= \frac{1}{\sqrt{2}} \int_0^\infty e^{x/\beta - x} L_k(x) f^S(\sqrt{x}) \, dx \\
&= \int_0^\infty \mu^{1-2/\beta}(r) \psi_{k,\beta}^S(r) f^S(r) r \, dr, \\
a_{k,\beta}^K &= \frac{1}{\sqrt{2}} \frac{1}{\sqrt{k+1}} \int_0^\infty e^{x/\beta - x} \sqrt{x} L_k^{(1)}(x) f^K(\sqrt{x}) \, dx \\
&= \int_0^\infty \mu^{1-2/\beta}(r) \psi_{k,\beta}^K(r) f^K(r) r \, dr.
\end{aligned}
$$

and $|a_{k,\beta}^S|, |a_{k,\beta}^K| \leqslant 2C(b) \sqrt{k+1} \, e^{-2b\sqrt{k}}$.

Proof. It is clear that both f^S and $\frac{1}{r} f^K$ are even and analytic. Moreover, owing to (2.12), we see that the functions

$$e^{r^2/\beta} f^S(r), \qquad e^{r^2/\beta} \frac{1}{r} f^K(r)$$

both satisfy the assumptions of Proposition 2.1. Thus, we have

$$e^{r^2/\beta} f^S(r) = \sum_{k=0}^{\infty} a_k^S L_k(r^2), \qquad e^{r^2/\beta} \frac{1}{r} f^K(r) = \sum_{k=0}^{\infty} \tilde{a}_k^K L_k^{(1)}(r^2),$$

which gives (2.13) with $a_k^K = \tilde{a}_k^K \sqrt{k+1}$. The expressions for a_k^S and a_k^K as well as their decay follow directly from Proposition 2.1. $\qquad \square$

As an immediate consequence of the orthonormality of the expansion systems we obtain approximation estimates for the truncated series in the weighted norm

$$\|f\|_\beta^2 := \int_0^\infty |f(r)|^2 e^{-(1-2/\beta)r^2} r \, dr :$$

COROLLARY 2.1 Under the assumptions of Proposition 2.2 we find for both $* = S$ and $* = K$

$$\left\| f^* - \sum_{k=0}^{K} a_{k,\beta}^* \psi_{k,\beta}^* \right\|_\beta \leqslant C'(b) K^{3/2} e^{-2b\sqrt{K}} \quad \text{for all } K \in \mathbb{N},$$

with a constant $C'(b) > 0$ depending only on b and independent of K, f, and β.

Let us now take the step to two dimensions, and consider an analytic function $f : \mathbb{R}^2 \to \mathbb{R}$. Associated with f are its even and odd parts,

$$f^S(r,\theta) = \frac{1}{2}\left(f(r,\theta) + f(r,\theta+\pi)\right), \qquad f^K(r,\theta) = \frac{1}{2}\left(f(r,\theta) - f(r,\theta+\pi)\right),$$

which are also both analytic. Fixing θ (effectively considering it a parameter), and assuming that f^S and f^K satisfy the conditions of Proposition 2.2 for some $\beta > 0$, we can write

$$f^S(r,\theta) = \sum_{k=0}^{\infty} a_{k,\beta}^S(\theta)\psi_{k,\beta}^S(r), \qquad f^K(r,\theta) = \sum_{k=0}^{\infty} a_{k,\beta}^K(\theta)\psi_{k,\beta}^K(r),$$

where a^S and a^K are rapidly decaying in k. In fact, as f^S is π-periodic in θ, we should be able to approximate $a_{k,\beta}^S(\theta)$ in terms of the complex exponentials ξ_l from (2.2) for *even* l, and correspondingly $a_{k,\beta}^K(\theta)$ in terms of ξ_l for *odd* l.

To simplify notation, let us introduce the notation for radial components of the basis functions

$$\varphi_k^{(\beta)} = \begin{cases} \psi_{k/2,\,\beta}^S, & \text{for even } k\,, \\ \psi_{(k-1)/2,\,\beta}^K, & \text{for odd } k\,, \end{cases} \tag{2.14}$$

so that we may write

$$f(r,\theta) = f^S(r,\theta) + f^K(r,\theta) = \sum_{k=0}^{\infty} a_k^{(\beta)}(\theta)\varphi_k^{(\beta)}(r),$$

where a_k corresponds to $a_{k/2,\beta}^S$ for even k and to $a_{(k-1)/2,\beta}^K$ for odd k, and where a_k has the same parity as k, i.e. $a_k(\theta+\pi) = (-1)^k a_k(\theta)$.

Continuing from before, we now write

$$a_k^{(\beta)}(\theta) = \sum_{2\,|\,(k-l)} F_{k,l}^{(\beta)}\xi_l(\theta),$$

where the complex coefficients are given by

$$F_{k,l}^{(\beta)} = \frac{1}{2\pi}\int_0^{2\pi} a_k^{(\beta)}(\theta)\xi_{-l}(\theta)\,d\theta.$$

Let us first consider even k. Then

$$\begin{aligned} F_{k,l}^{(\beta)} &= \frac{1}{2\pi}\int_0^{2\pi}\int_0^{\infty} \mu^{1-2/\beta}(r)\varphi_k^{(\beta)}(r)\xi_{-l}(\theta)f^S(r,\theta)\,r\,dr\,d\theta \\ &= \frac{1}{2\pi}\int_{\mathbb{R}^2}\mu^{1-2/\beta}(r)\varphi_k^{(\beta)}(r)\xi_{-l}(\theta)f^S(\nu)\,d\nu = \frac{1}{2\pi}\int_{\mathbb{R}^2}\mu^{1-2/\beta}(r)\varphi_k^{(\beta)}(r)\xi_{-l}(\theta)f(\nu)\,d\nu, \end{aligned}$$

since ξ_{-l} is even, the corresponding integral with f^K will be zero. Precisely the same argument applies for k odd. Thus, we arrive at

$$\boxed{f(r,\theta) = \sum_{2\,|\,(k-l)} F_{k,l}^{(\beta)}\,\varphi_k^{(\beta)}(r)\xi_l(\theta)\,,} \tag{2.15}$$

with complex coefficients

$$F_{k,l}^{(\beta)} = \frac{1}{2\pi} \int_{\mathbb{R}^2} \mu^{1-2/\beta}(r) \varphi_k^{(\beta)}(r) \xi_{-l}(\theta) f(\boldsymbol{v}) \, \mathrm{d}\boldsymbol{v}.$$

We will use the notation $L^2(\mathbb{R}^2; \beta)$ to denote a weighted L^2-space with inner product

$$\langle f, g \rangle_{L^2(\mathbb{R}^2;\beta)} = \frac{1}{2\pi} \int_{\mathbb{R}^2} \mu^{1-2/\beta}(r) f(\boldsymbol{v}) \bar{g}(\boldsymbol{v}) \, \mathrm{d}\boldsymbol{v}. \tag{2.16}$$

We retain the notation $\|f\|_\beta$ for the induced norm. We also note in passing that $L^2(\mathbb{R}^2; 2) = L^2(\mathbb{R}^2)$ We note that the functions $\varphi_k^{(\beta)} \xi_l$ form a complete orthonormal system with respect to the weight $\frac{1}{2\pi} \mu^{1-2/\beta}$. For $\beta = 2$ we even have orthogonality with respect to the usual Lebesgue measure:

PROPOSITION 2.3 Assuming $k_1 \equiv l_1 \pmod 2$ and $k_2 \equiv l_2 \pmod 2$, we have

$$\left\langle \varphi_{k_1}^{(\beta)} \xi_{l_1}, \varphi_{k_2}^{(\beta)} \xi_{l_2} \right\rangle_{L^2(\mathbb{R}^2;\beta)} = \frac{1}{2\pi} \int_{\mathbb{R}^2} \mu^{1-2/\beta} \varphi_{k_1}^{(\beta)} \xi_{l_1} \varphi_{k_2}^{(\beta)} \xi_{-l_2} \, \mathrm{d}\boldsymbol{v} = \delta_{k_1,k_2} \delta_{l_2,l_2}.$$

Proof. First, we note that if k_1 and k_2 have different parities, the integrand is odd, and so the integral is zero. Thus, we assume from now that they have equal parities. We have

$$\begin{aligned}
\left\langle \varphi_{k_1}^{(\beta)} \xi_{l_1}, \varphi_{k_2}^{(\beta)} \xi_{l_2} \right\rangle_{L^2(\mathbb{R}^2;\beta)} &= \frac{1}{2\pi} \int_0^{2\pi} \xi_{l_1-l_2} \, \mathrm{d}\theta \int_0^\infty \mu^{1-2/\beta} \varphi_{k_1}^{(\beta)} \varphi_{k_2}^{(\beta)} \, r \, \mathrm{d}r \\
&= \delta_{l_1,l_2} \int_0^\infty \mu^{1-2/\beta} \varphi_{k_1}^{(\beta)} \varphi_{k_2}^{(\beta)} \, r \, \mathrm{d}r
\end{aligned}$$

For k_1, k_2 both even, we have

$$\begin{aligned}
\int_0^\infty \mu^{1-2/\beta} \varphi_{k_1}^{(\beta)} \varphi_{k_2}^{(\beta)} r \, \mathrm{d}r &= \int_0^\infty \mathrm{e}^{-r^2} L_{k_1/2}(r^2) L_{k_2/2}(r^2) \, 2r \, \mathrm{d}r \\
&= \int_0^\infty \mathrm{e}^{-x} L_{k_1/2}(x) L_{k_2/2}(x) \, \mathrm{d}x \overset{(2.8)}{=} \frac{1}{2} \delta_{k_1,k_2}.
\end{aligned}$$

And for k_1, k_2 both odd, we find, using $Z(a,b) = [(a+1)(b+1)]^{-1/2}$,

$$\begin{aligned}
\int_0^\infty \mu^{1-2/\beta} \varphi_{k_1}^{(\beta)} \varphi_{k_2}^{(\beta)} r \, \mathrm{d}r &= 2Z(k_1,k_2) \int_0^\infty \mathrm{e}^{-r^2} r^2 L_{(k_1-1)/2}^{(1)}(r^2) L_{(k_2-1)/2}^{(1)}(r^2) \, r \, \mathrm{d}r \\
&= Z(k_1,k_2) \int_0^\infty \mathrm{e}^{-x} x L_{(k_1-1)/2}^{(1)}(x) L_{(k_2-1)/2}^{(1)}(x) \, \mathrm{d}x \\
&\overset{(2.8)}{=} \delta_{k_1,k_2}.
\end{aligned}$$

This concludes the proof. $\qquad\square$

For $K, L, \beta > 0$ and L even, we define the *KL*-dimensional function spaces of complex valued functions $\mathbb{R}^2 \mapsto \mathbb{C}$:

$$V_\beta(K,L) = \mathrm{span}\left\{ \varphi_k^{(\beta)} \xi_l \ : \ 0 \leqslant k < K, \ -L \leqslant l < L, \ k \equiv l \pmod 2 \right\} \tag{2.17}$$

As basis we use the polar tensor product functions

$$\mathscr{B}_\beta(K,L) := \left\{ \varphi_k^{(\beta)} \xi_l \ : \ 0 \leqslant k < K, \ -L \leqslant l < L, \ k \equiv l \,(\mathrm{mod}\,2) \right\} . \tag{2.18}$$

The requirement that L is even is made for the sake of simplicity, as the basis functions can now be enumerated as $b_{k,q} = \varphi_k \xi_{l(q,k)}$ for $0 \leqslant k < K$ and $0 \leqslant q < L$, where

$$l(q,k) = \begin{cases} 2q - (-1)^k, & q < L/2 \\ 2(q-L) - (-1)^k, & \text{otherwise.} \end{cases} \tag{2.19}$$

Let us also denote by $P_{V_\beta(K,L)}$ (or, when convenient, merely P_V) the $L^2(\mathbb{R}^2;\beta)$-orthogonal projection onto $V_\beta(K,L)$. Next, we combine the estimate of Corollary 2.1 and well-known results about the approximation of analytic functions by means of trigonometric polynomials into a result about best approximation in $V_\beta(K,L)$.

COROLLARY 2.2 Let $f : \mathbb{R}^2 \mapsto \mathbb{R}$, viewed as a function $f = f(r,\theta)$ of polar coordinates, possess an analytic extension to the tensor product strip $s(c) \times s(\gamma^2) \subset \mathbb{C}^2$ with $c, \gamma > 0$ and $s(\cdot)$ defined in (2.9). Then, for any $0 < b < c$ and $0 < \rho < \gamma$,

$$\left\| f - P_{V_\beta(K,L)} f \right\|_\beta \leqslant C(b,\rho) K^{3/2} \mathrm{e}^{-2b\sqrt{K} - \rho L} ,$$

with a constant $C = C(b,\rho) > 0$ independent of K, L, f, and β.

We propose a Galerkin discretization of (1.1) in velocity space based on the trial and test space V and the inner product (2.16). This means that, given an initial condition $f_0(\boldsymbol{v})$, we solve (1.1) approximately in the form of the projected equation for $f_V \in C^\infty([0,T],V)$, $T > 0$ final time,

$$\frac{\partial f_V}{\partial t} = P_V Q(f_V, f_V) \quad , \quad f_V(0) = P_V f_0. \tag{2.20}$$

This is equivalent to a non-linear ordinary differential equation for the complex expansion coefficients of f_V, cf. (2.15). The evolution (2.20) amounts to the semi-discrete and non-adaptive version of our method. It is worth noting that unlike the Fourier method, we need not truncate the collision operator. Thus we avoid all the aliasing effects which plague the conventional Fourier methods.

3. Equilibria and initial values

3.1 *Adapted solutions*

The space $V_\beta(K,L)$ contains functions on the form

$$\varphi_0^{(\beta)} \xi_0 = \exp(-\|\boldsymbol{v}\|^2/\beta),$$

which are equilibrium solutions with mass $\beta\pi$, momentum $\boldsymbol{0}$ and temperature $\beta/2$. Thus, if the initial condition conforms to these conditions, we can expect that for k,l not both zero, the corresponding time-dependent coefficient $F_{k,l}^{(\beta)}(t)$ in the expansion (2.15) of F_V from (2.20) tends to zero for $t \to \infty$. If the initial condition does not match this particular mass, momentum and temperature, the equilibrium solution cannot be exactly represented in any of the finite-dimensional spaces $V_\beta(K,L)$. However, owing to the equilibrium solution being isotropic, its polar representation (2.15) will still have zero coefficients for all $l \neq 0$. Thus, we expect $F_{k,l}^{(\beta)}(t)$ to tend to zero for all $l \neq 0$ for $t \to \infty$.

DEFINITION 3.1 We say that a function $f(\mathbf{v})$ is β-*conforming* if mass, momentum, and temperature attain the particular values

$$\rho(f) = \beta\pi, \qquad \mathbf{u}(f) = \mathbf{0}, \qquad T(f) = \frac{\beta}{2}.$$

THEOREM 3.2 Let $g(t,\mathbf{v})$ be a solution to (1.1), where the collision kernel B satisfies Assumption 1.2. Let $\alpha, \gamma > 0$ be given, and define $\eta = \alpha/\gamma^{\lambda+2}$. Then

$$h(t,\mathbf{v}) = \alpha g(\eta t, \gamma\mathbf{v})$$

is also a solution to (1.1).

Proof. First,

$$\begin{aligned}
\frac{\partial h}{\partial t}(t,\mathbf{v}) &= \alpha\eta\frac{\partial g}{\partial t}(\eta t, \gamma\mathbf{v}) \\
&= \alpha\eta \int_{\mathbb{R}^2}\int_{\mathbb{S}^1} \|\gamma\mathbf{v} - \bar{\mathbf{v}}_*\|^\lambda b(\cos\theta) \\
&\qquad\qquad \left[g(\eta t, \bar{\mathbf{v}}')g(\eta t, \bar{\mathbf{v}}_*') - g(\eta t, \gamma\mathbf{v})g(\eta t, \bar{\mathbf{v}}_*) \right] \, \mathrm{d}\boldsymbol{\sigma} \, \mathrm{d}\bar{\mathbf{v}}_*,
\end{aligned}$$

where the collision identities read

$$\bar{\mathbf{v}}', \bar{\mathbf{v}}_*' = \frac{1}{2}\left(\gamma\mathbf{v} + \bar{\mathbf{v}}_* \pm \|\gamma\mathbf{v} - \bar{\mathbf{v}}_*\|\boldsymbol{\sigma} \right).$$

Making the change of variables $\bar{\mathbf{v}}_*, \bar{\mathbf{v}}', \bar{\mathbf{v}}_*' = \gamma\mathbf{v}_*, \gamma\mathbf{v}', \gamma\mathbf{v}_*'$, we recover the familiar collision identity

$$\mathbf{v}', \mathbf{v}_*' = \frac{1}{2}\left(\mathbf{v} + \mathbf{v}_* \pm \|\mathbf{v} - \mathbf{v}_*\|\boldsymbol{\sigma} \right),$$

whence

$$\begin{aligned}
\frac{\partial h}{\partial t}(t,\mathbf{v}) &= \alpha\eta \int_{\mathbb{R}^2}\int_{\mathbb{S}^1} \|\gamma\mathbf{v} - \gamma\mathbf{v}_*\|^\lambda b(\cos\theta) \\
&\qquad\qquad \left[g(\eta t, \gamma\mathbf{v})g(\eta t, \gamma\mathbf{v}_*') - g(\eta t, \gamma\mathbf{v})g(\eta t, \gamma\mathbf{v}_*) \right] \, \mathrm{d}\boldsymbol{\sigma} \, \mathrm{d}(\gamma\mathbf{v}_*) \\
&= \frac{\eta\gamma^{\lambda+2}}{\alpha} Q(h,h)(\mathbf{v}).
\end{aligned}$$

Since $\eta\gamma^{\lambda+2}/\alpha = 1$, this concludes the proof. $\qquad\square$

REMARK 3.1 A corresponding result holds in arbitrary dimensions d, where $\eta = \alpha/\gamma^{\lambda+d}$.

Hence, the "problem" of nonconforming initial values is easily overcome. Theorem 3.2 allows us to transform any initial condition $f(0,\mathbf{v})$ to become β-conforming. Then we solve it in the space $\mathscr{P}_\beta(K,L)$, and afterwards we recover the solution, as demonstrated in the following theorem. This makes it possible to reuse the same Galerkin discretization of the collision operator for different values of observables.

THEOREM 3.3 Let $f(t,\mathbf{v})$ be a solution to (1.1), where B satisfies Assumption 1.2. Let $\beta > 0$ be given, and assume f has mass, momentum and temperature ρ, $\mathbf{u}$ and T. Define

$$\gamma = \sqrt{\frac{2T}{\beta}}, \qquad \alpha = \frac{2\pi T}{\rho}, \qquad \eta = \frac{\alpha}{\gamma^{\lambda+2}}. \tag{3.1}$$

Then

$$h(t, \boldsymbol{v}) = \alpha f(\eta t, \gamma \boldsymbol{v} + \boldsymbol{u})$$

is a β-conforming solution to (1.1), and f can be recovered via $f(t, \boldsymbol{v}) = \alpha^{-1} h(t/\eta, (\boldsymbol{v} - \boldsymbol{u})/\gamma)$.

Proof. We show that h is β-conforming. Indeed,

$$\rho(h) = \alpha \int_{\mathbb{R}^2} f(\gamma \boldsymbol{v} + \boldsymbol{u}) \, d\boldsymbol{v} = \frac{\alpha}{\gamma^2} \int_{\mathbb{R}^2} f(\gamma \boldsymbol{v} + \boldsymbol{u}) \, d(\gamma \boldsymbol{v} + \boldsymbol{u}) = \frac{\alpha}{\gamma^2} \rho, \tag{3.2}$$

and

$$\begin{aligned}
T(h) &= \frac{1}{2\rho(h)} \int_{\mathbb{R}^2} \alpha f(\gamma \boldsymbol{v} + \boldsymbol{u}) \, d\boldsymbol{v} = \frac{1}{2\gamma^2 \rho} \int_{\mathbb{R}^2} f(\boldsymbol{s}) \|\boldsymbol{s} - \boldsymbol{u}\|^2 \, d\boldsymbol{s} \\
&= \frac{1}{2\gamma^2 \rho} \left[\int_{\mathbb{R}^2} f(\boldsymbol{s}) \|\boldsymbol{s}\|^2 \, d\boldsymbol{s} + \|\boldsymbol{u}\|^2 \int_{\mathbb{R}^2} f(\boldsymbol{s}) \, d\boldsymbol{s} - 2\boldsymbol{u} \cdot \int_{\mathbb{R}^2} f(\boldsymbol{s}) \boldsymbol{s} \, d\boldsymbol{s} \right] \\
&= \frac{1}{2\gamma^2} \left[E + \|\boldsymbol{u}\|^2 - 2\|\boldsymbol{u}\|^2 \right] = \frac{1}{\gamma^2} T. \tag{3.3}
\end{aligned}$$

Setting $\rho(h) = \beta \pi$ and $T(h) = \beta/2$, and solving (3.2)-(3.3) for α, γ, we find precisely (3.1). It is easy to see that $\boldsymbol{u}(h) = \boldsymbol{0}$. That h is a solution of (1.1) immediately follows from Theorems 1.1 and 3.2. $\square$

3.2 *Choice of Decay Parameter β*

The properties of the bases $\mathscr{B}_\beta$ heavily depend on the value of β. We have already noted that for $\beta = 2$, the weighted inner product $\langle \cdot, \cdot \rangle_{L^2(\mathbb{R}^2; \beta)}$ becomes the standard L^2 inner product, and so error analysis in familiar norms will be simple.

REMARK 3.2 There is empiric evidence that for solutions f of (1.1), the expansion coefficients $F_{k,l}^{(\beta)}(t)$ decay fastest, in terms of k, for $\beta = 2$. As a consequence one can consistently achieve faster convergence for $\beta = 2$ than for $\beta < 2$, both in the weighted norm and the L^2-norm.

A key selection criterion for β is the stability of the bases with respect to the observables.

THEOREM 3.4 Let $\beta > 0$ be given and define the linear functionals[1]

$$\rho(f) = \int_{\mathbb{R}^2} f(\boldsymbol{v}) \, d\boldsymbol{v} \text{ (mass)}, \quad (\boldsymbol{u}\rho)(f) = \int_{\mathbb{R}^2} f(\boldsymbol{v}) \boldsymbol{v} \, d\boldsymbol{v} \text{ (momentum)},$$

$$(E\rho)(f) = \int_{\mathbb{R}^2} f(\boldsymbol{v}) \|\boldsymbol{v}\|^2 \, d\boldsymbol{v} \text{ (total energy)}.$$

These functionals attain the following values for particular functions in $\mathscr{B}_\beta(K, L)$:

$$\rho\left(\xi_0 \psi_{k,\beta}^S \right) = \sqrt{2} \beta \pi (1 - \beta)^k,$$

$$(\boldsymbol{u}\rho)\left(\xi_{\pm 1} \psi_{k,\beta}^K \right) = \frac{1}{\sqrt{2}} \begin{pmatrix} 1 \\ \pm i \end{pmatrix} \beta^2 \pi \sqrt{k+1} (1 - \beta)^k,$$

$$(E\rho)\left(\xi_0 \psi_{k,\beta}^S \right) = \sqrt{2} \beta^2 \pi \cdot \begin{cases} [1 - (k+1)\beta](1 - \beta)^{k-1}, & k > 0, \\ 1, & k = 0, \end{cases}$$

---

[1] Here we have abused notation somewhat, since the quantity $(E\rho)(f)$ as defined above is only equal to $E(f)\rho(f)$ if $\rho(f) \neq 0$, and similarly for $\boldsymbol{u}\rho$.

using the convention that $0^0 = 1$ if $\beta = 1$. For all other products of ξ_l and $\psi_{k,\beta}^*$ in the basis $\mathscr{B}_\beta(K,L)$ the functionals evaluate to zero.

Proof. The proof for this is not difficult, but it involves a fair amount of algebra. First, we have the expansion of Laguerre polynomials in terms of monomials,

$$L_k^{(\alpha)}(x) = \sum_{i=0}^{k} \binom{k+\alpha}{k-i} \frac{(-1)^i}{i!} x^i.$$

For mass and energy, we first note that any integration against ξ_l for $l \neq 0$ must yield zero. For momentum, note that (considering $\boldsymbol{v}$ as a complex number) we have $\boldsymbol{v} = \binom{r\cos\theta}{r\sin\theta}$, so any integration against $\xi_l(\boldsymbol{v}) = e^{il\theta}$ for $l \neq \pm 1$ must yield zero.

Thus, for mass we have

$$\frac{1}{\sqrt{2}} \rho\left(\xi_0 \psi_{k,\beta}^S\right) = 2\pi \int_0^\infty e^{-r^2/\beta} L_k(r^2)\, r\,dr = \beta\pi \int_0^\infty e^{-u} L_k(\beta u)\,du$$

$$= \beta\pi \int_0^\infty e^{-u} \sum_{i=0}^{k} \binom{k}{i} \frac{(-1)^i}{i!} (\beta u)^i\,du$$

$$= \beta\pi \sum_{i=0}^{k} \binom{k}{i} \frac{(-\beta)^i}{i!} \underbrace{\int_0^\infty e^{-u} u^i\,du}_{=\Gamma(i+1)=i!}$$

$$= \beta\pi \sum_{i=0}^{k} \binom{k}{i} (-\beta)^i 1^{k-i} = \beta\pi(1-\beta)^k.$$

For the total energy functional the technique is mostly the same, except one needs the identity $\binom{k}{i} = \frac{k}{i}\binom{k-1}{i-1}$ for $k,i > 0$. Thus, for $k > 0$ we find

$$\frac{1}{\sqrt{2}}(E\rho)\left(\xi_0 \psi_{k,\beta}^S\right) = 2\pi \int_0^\infty e^{-r^2/\beta} r^2 L_k(r^2)\, r\,dr = \beta^2\pi \int_0^\infty e^{-u} u L_k(\beta u)\,du$$

$$= \beta^2\pi \int_0^\infty e^{-u} u \sum_{i=0}^{k} \binom{k}{i} \frac{(-1)^i}{i!} (\beta u)^i\,du$$

$$= \beta^2\pi \sum_{i=0}^{k} \binom{k}{i} \frac{(-\beta)^i}{i!} \int_0^\infty e^{-u} u^{i+1}\,du$$

$$= \beta^2\pi \sum_{i=0}^{k} \binom{k}{i} (i+1)(-\beta)^i$$

$$= \beta^2\pi \underbrace{\sum_{i=0}^{k} \binom{k}{i}(-\beta)^i}_{=(1-\beta)^k} + \beta^2\pi \sum_{i=1}^{k} \binom{k}{i} \underbrace{i\,(-\beta)^i}_{=k\binom{k-1}{i-1}}$$

$$= \beta^2\pi \left[(1-\beta)^k - \beta k \sum_{i=1}^{k} \binom{k-1}{i-1}(-\beta)^{i-1}\right]$$

$$= \beta^2\pi \left[(1-\beta)^k - \beta k (1-\beta)^{k-1}\right] = \beta^2\pi[1-(k+1)\beta](1-\beta)^{k-1}.$$

If $k = 0$ the second sum can be dropped, and one is left with $\beta^2 \pi$.

Lastly, momentum, where we consider only one component:

$$
\sqrt{\tfrac{k+1}{2}} \, (\boldsymbol{u}\rho)\left(\xi_{-1}\psi_{k,\beta}^{\mathrm{K}}\right) = \int_0^{2\pi}\int_0^\infty e^{-r^2/\beta} r^2 L_k^{(1)}(r^2)\xi_{-1}(\theta)\, r\cos(\theta)\,\mathrm{d}r = \pi \int_0^\infty e^{-r^2/\beta} r^2 L_k^{(1)}(r^2)\, r\,\mathrm{d}r
$$

$$
= \beta^2 \pi \int_0^\infty e^{-u} u L_k^{(1)}(\beta u)\,\mathrm{d}u = \beta^2\pi \int_0^\infty e^{-u} u \sum_{i=0}^k \binom{k+1}{k-i}(\beta u)^i\,\mathrm{d}u
$$

$$
= \beta^2\pi \sum_{i=0}^k \binom{k+1}{k-i}\frac{(-\beta)^i}{i!}\int_0^\infty e^{-u} u^{i+1}\,\mathrm{d}u = \beta^2\pi\sum_{i=0}^k \underbrace{\binom{k+1}{k-i}(i+1)(-\beta)^i}_{=(k+1)\binom{k}{i}}
$$

$$
= \beta^2\pi(k+1)\sum_{i=0}^k \binom{k}{i}(-\beta)^i = \beta^2\pi(k+1)(1-\beta)^k.
$$

<div align="right">□</div>

In particular, we arrive at the following asymptotic rates.

COROLLARY 3.1 It holds that

- for $0 < \beta < 2$ we have exponential decay of observables for basis functions as $k \to \infty$, i.e:

$$
\rho\left(\psi_{k,\beta}^{\mathrm{S}}\right) = (\boldsymbol{u}\rho)\left(\xi_{-1}\psi_{k,\beta}^{\mathrm{K}}\right) = (E\rho)\left(\psi_{k,\beta}^{\mathrm{S}}\right) \in \mathscr{O}(|\beta-1|^k).
$$

All these bases are stable with respect to observables.

- for $\beta = 1$ only a few basis functions contribute to the observables:

$$
\tfrac{1}{\sqrt{2}}\rho\left(\psi_{k,1}^{\mathrm{S}}\right) = \sqrt{2}(\boldsymbol{u}\rho)\left(\xi_{-1}\psi_{k,1}^{\mathrm{K}}\right) = \delta_{0,k}\pi \quad , \quad (E\rho)\left(\psi_{k,1}^{\mathrm{S}}\right) = \sqrt{2}\pi\begin{cases}1, & k=0,\\ -1, & k=1,\\ 0, & k\geqslant 2.\end{cases}
$$

- for $\beta = 2$ we have polynomial instability:

$$
\rho\left(\psi_{k,\beta}^{\mathrm{S}}\right) \in \mathscr{O}(1), \qquad (\boldsymbol{u}\rho)\left(\xi_{-1}\psi_{k,\beta}^{\mathrm{K}}\right) = (E\rho)\left(\psi_{k,\beta}^{\mathrm{S}}\right) \in \mathscr{O}(k).
$$

- for $\beta > 2$ we have exponential instability:

$$
\rho\left(\psi_{k,\beta}^{\mathrm{S}}\right) = (\boldsymbol{u}\rho)\left(\xi_{-1}\psi_{k,\beta}^{\mathrm{K}}\right) = (E\rho)\left(\psi_{k,\beta}^{\mathrm{S}}\right) \in \mathscr{O}((\beta-1)^k).
$$

In a sense, $\beta = 1$ is optimal, because we have exact conservation of **all** observable in the semi-discrete evolution.

THEOREM 3.5 If $\beta = 1$, then mass, momentum, and total energy as defined in Theorem 3.4 are invariants of the semi-discrete evolution (2.20)

Proof. (i) In (2.20) choose the test function $g := \frac{1}{\sqrt{2}}\xi_0\psi_{0,1}^S$, that is $g(r,\theta) = e^{-r^2}$. The weight in the inner product exactly offsets the factor e^{-r^2}. Thus we end up with

$$\frac{d}{dt}\langle f_V, g\rangle_{L^2(\mathbb{R}^2;1)} = \frac{d}{dt}\int_{\mathbb{R}^2} f_V(\boldsymbol{v})\,d\boldsymbol{v} = \frac{d}{dt}\rho(f_V) = \int_{\mathbb{R}^2} Q(f_V, f_V)\,d\boldsymbol{v} = 0\,,$$

by fundamental conservation properties of the Boltzmann collision operator (Cercignani, 2002, Sect. 5).

(ii) We choose the test functions $\xi_{\pm 1}\psi_{0,1}^K$ and note that $g_1 := \sqrt{\frac{k+1}{8}}(\xi_1 + \xi_{-1})\psi_{0,1}^K = \cos(\theta)re^{-r^2}$ and $g_2 := \frac{1}{i}\sqrt{\frac{k+1}{8}}(\xi_1 + \xi_{-1})\psi_{0,1}^K = \sin(\theta)re^{-r^2}$. Hence, again we benefit from a cancellation of the weights and (2.20) involves

$$\frac{d}{dt}\left\langle f_V, \begin{pmatrix} g_1 \\ g_2 \end{pmatrix}\right\rangle_{L^2(\mathbb{R}^2;1)} = \frac{d}{dt}(\boldsymbol{u}\rho)(f_V) = \int_{\mathbb{R}^2} Q(f_V, f_V)\,\boldsymbol{v}\,d\boldsymbol{v} = 0\,.$$

(iii) Finally, the test function $g := \frac{1}{\sqrt{2}}\xi_0(\psi_{0,1}^S - \psi_{1,1}^S)$ evaluates to $g(\boldsymbol{v}) = \|\boldsymbol{v}\|^2 e^{-r^2}$, which means

$$\frac{d}{dt}\langle f_V, g\rangle_{L^2(\mathbb{R}^2;1)} = \frac{d}{dt}(E\rho))(f_V) = \int_{\mathbb{R}^2} Q(f_V, f_V)\,\|\boldsymbol{v}\|^2\,d\boldsymbol{v} = 0\,.$$

$\square$

The last detail to keep in mind is that any $\beta > 2$ results in an unbounded basis, that is

$$\sup_k \sup_r \left|\varphi_k^{(\beta)}(r)\right| = \infty.$$

This fact follows from the following asymptotic expression (Gavrilyuk & Khoromskij, 2011, Equation 2.12):

$$L_k^{(\alpha)}(x) = \pi^{-1/2}e^{x/2}x^{-\alpha/2-1/4}k^{\alpha/2-1/4}\left[\cos\left(2\sqrt{kx} - \omega\pi\right) + \mathscr{O}\left(k^{-1/2}\right)\right],$$

for some ω depending on α, but not on x or k.

In summary, $\beta = 2$ seems to somewhat faster convergence in the L^2-norm and easier analysis in this norm, while $\beta = 1$ guarantees exact conservation of all observables. One might also employ a value $1 < \beta < 2$ as a compromise, while values $\beta > 2$ render the basis useless for numerical purposes.

In this paper we have only performed experiments with $\beta \in \{1,2\}$. No other values will be considered in Section 5.

4. Computational Aspects

4.1 *Evaluating Discrete Collision Operators*

We now turn to the practical aspects of evaluating $Q(f,g)$ for $f,g \in V_\beta(K,L)$. Taking the $L^2(\mathbb{R}^2;\beta)$-orthogonal approximation by discarding the extra coefficients, we have, due to bilinearity of Q,

$$Q(f,g) = \sum_{k,l}\left(\sum_{k_1,k_2,l_1,l_2} S_{k_1,k_2,l_1,l_2}^{k,l}F_{k_1,l_1}^{(\beta)}G_{k_2,l_2}^{(\beta)}\right)\varphi_k^{(\beta)}\xi_l, \tag{4.1}$$

in a formal sense and $F_{k,l}^{(\beta)}, G_{k,l}^{(\beta)}$ are the coefficients for f and g respectively (according to (2.15)), and

$$S_{k_1,k_2,l_1,l_2}^{k,l} = \left\langle Q\left(\varphi_{k_1}^{(\beta)}\xi_{l_1}, \varphi_{k_2}^{(\beta)}\xi_{l_2}\right), \varphi_k^{(\beta)}\xi_l \right\rangle_{L^2(\mathbb{R}^2;\beta)}.$$

Of course, the entries of the tensor S also depend on β, but we have suppressed this. S is K^3L^3-dimensional, and forming a sum such as (4.1) at each timestep is extremely expensive. However, some effort can be saved by exploiting convolution structure, which is revealed by the following corollary of Theorem 1.1.

COROLLARY 4.1 Let f and g be represented in polar coordinates as

$$f(r,\theta) = f_r(r)e^{ik\theta}, \qquad g(r,\theta) = g_r(r)e^{il\theta},$$

for some functions f_r, g_r, k and l. Then,

$$Q(f,g)(r,\theta) = C(r)e^{i(k+l)\theta}$$

for some function C depending on f_r, g_r, k and l.

Proof. Let ρ_ω be a rotation operator through ω, that is

$$\rho_\omega f(r,\theta) = f(r,\theta - \omega)$$

We get $\rho_\omega f = e^{-ik\omega}f$, and correspondingly for g. Using Theorem 1.1 and the linearity of Q we obtain

$$\rho_\omega Q(f,g)(r,\theta) = e^{-i(k+l)\omega}Q(f,g)(r,\theta).$$

Choose $\omega = \theta$ and rearrange to find

$$Q(f,g)(r,\theta) = e^{i(k+l)\theta}\rho_\theta Q(f,g)(r,\theta).$$

The result follows since $\rho_\theta Q(f,g)(r,\theta) = Q(f,g)(r,0)$ is independent of θ.   □ By Corollary 4.1, S is nonzero only for $l_1 + l_2 = l$, reducing the complexity to K^3L^2. Assuming $K = L = N$ degrees of freedom in each direction, and generalizing to arbitrary dimensions, this yields a complexity of "only" N^{2d+1} compared to the N^{2d} of the simple Fourier spectral discretization.

REMARK 4.1 At first glance, the computational effort involved in the polar spectral method appears to be daunting. However, we point out that the basis functions from (2.18) combined with the rescaling discussed in Section 3.1 are particularly well adapted to the structure of the solutions of (1.1), since for $t \to \infty$ the solution will converge to a single basis function. This immediately suggests effective adaptive strategies, which will greatly reduce the required number of degrees of freedom at later times.

In detail, to take advantage of the expected exponential decay in time of all basis expansion coefficients $F_{k,l}$ except $k = l = 0$, we have implemented a simple adaptive scheme reducing the number of degrees of freedom when coefficients reach a threshold value.

As we will see in the numerical experiments, coefficients go to zero in an order which is primarily determined by l. That is, in general, F_{k_1,l_1} will reach a threshold value before F_{k_2,l_2} if $|l_1| > |l_2|$.

This suggests the following simple adaptivity check: after every timestep, check the magnitude of the coefficients $F_{k,l}$ with $l \in \{-L, -L+1, L-1, L-2\}$. If they are all below the threshold, reduce L by 2.

REMARK 4.2 The core challenge when generalizing this method to higher dimensions is to find an analogue of Corollary 4.1 for $d > 2$. The problem of rotating expansions in spherical harmonics is non-trivial. The classical text is Wigner (1944). For more recent work, see for example Ivanic & Ruedenberg (1996) (real spherical harmonics) and Lessig *et al.* (2012).

At least, what can be said is that these rotation operators are band-restricted, so that a rotated spherical harmonic Y_l^m contains no contributions from harmonics with degrees different from l.

4.2 *Computing the discrete collision operator*

Let us now turn to the issue of evaluating the coefficients of K. For this, we will split the operator into gain and loss parts, and first consider the **loss part**. With $\varphi_k^{(\beta)}$ defined in (2.14)

$$
\begin{aligned}
S_{k_1,k_2,l_1,l_2}^{k,l\,(-)} &= \left\langle Q^- \left(\varphi_{k_1}^{(\beta)} \xi_{l_1}, \varphi_{k_2}^{(\beta)} \xi_{l_2} \right), \varphi_k^{(\beta)} \xi_l \right\rangle_{L^2(\mathbb{R}^2;\beta)} \\
&= \frac{1}{\pi} \int_{\mathbb{R}^2} \int_{\mathbb{R}^2} \int_{\mathbb{S}^1} B(\|\boldsymbol{v} - \boldsymbol{v}_*\|, \cos\theta) \\
&\qquad\qquad \left(\mu^{1-2/\beta} \varphi_{k_1}^{(\beta)} \xi_{l_1} \varphi_k^{(\beta)} \xi_{-l} \right)(\boldsymbol{v}) \left(\varphi_{k_2}^{(\beta)} \xi_{l_2} \right)(\boldsymbol{v}_*) \, \mathrm{d}\boldsymbol{\sigma} \, \mathrm{d}\boldsymbol{v}_* \, \mathrm{d}\boldsymbol{v} \\
&= \frac{1}{\pi} \int_{\mathbb{R}^2} \left(\mu^{1-2/\beta} \varphi_{k_1}^{(\beta)} \xi_{l_1} \varphi_k^{(\beta)} \xi_{-l} \right)(\boldsymbol{v}) \int_{\mathbb{R}^2} \left(\varphi_{k_2}^{(\beta)} \xi_{l_2} \right)(\boldsymbol{v}_*) \mathscr{I}^-(\boldsymbol{v}, \boldsymbol{v}_*) \, \mathrm{d}\boldsymbol{v}_* \, \mathrm{d}\boldsymbol{v},
\end{aligned}
$$

where the *inner integral* $\mathscr{I}^-$ is given by

$$
\mathscr{I}^-(\boldsymbol{v}, \boldsymbol{v}_*) = \int_{\mathbb{S}^1} B(\|\boldsymbol{v} - \boldsymbol{v}_*\|, \cos\theta) \, \mathrm{d}\boldsymbol{\sigma} \ .
$$

It prevents us from separating the two integrals over $\mathbb{R}^2$ (It is generally not the case that $\mathscr{I}^-$ has low separation rank, so a corresponding strategy of simplification fails). However, $\mathscr{I}^-(\boldsymbol{v}, \boldsymbol{v}_*)$ *is a function of just one real variable*, namely $\|\boldsymbol{v} - \boldsymbol{v}_*\|$. In fact, by Assumption 1.2, we have

$$
\mathscr{I}^-(\boldsymbol{v}, \boldsymbol{v}_*) = \|\boldsymbol{v} - \boldsymbol{v}_*\|^\lambda \int_{\mathbb{S}^1} b(\cos\theta) \, \mathrm{d}\boldsymbol{\sigma}.
$$

Hence, quadrature is cheap. Then the value of $\mathscr{I}^-(\boldsymbol{v}, \boldsymbol{v}_*)$ for pairs of quadrature points in velocity is readily available.

REMARK 4.3 For the Maxwellian kernel, $B \equiv 1/2\pi$, the loss part is particularly easy to evaluate, as $\mathscr{I}^- \equiv 1$, giving

$$
\begin{aligned}
S_{k_1,k_2,l_1,l_2}^{k,l\,(-)} &= \frac{1}{2\pi} \int_{\mathbb{R}^2} \left(\mu^{1-2/\beta} \varphi_{k_1}^{(\beta)} \xi_{l_1} \varphi_k^{(\beta)} \xi_{-l} \right) \mathrm{d}\boldsymbol{v} \int_{\mathbb{R}^2} \left(\varphi_{k_2}^{(\beta)} \xi_{l_2} \right) \mathrm{d}\boldsymbol{v}_* \\
&= \frac{1}{2\pi} \left\langle \varphi_{k_1}^{(\beta)} \xi_{l_1}, \varphi_k^{(\beta)} \xi_l \right\rangle_{L^2(\mathbb{R}^2;\beta)} \rho \left(\varphi_{k_2}^{(\beta)} \xi_{l_2} \right) \\
&= \delta_{k,k_1} \, \delta_{l,l_1} \, \delta_{0,l_2} \, \rho \left(\varphi_{k_2}^{(\beta)} \right)
\end{aligned}
$$

Theorem 3.4 provides the values for the masses $\rho \left(\varphi_{k_2}^{(\beta)} \right)$.

Let us now turn to the **gain part**. In a similar vein as before, we find

$$S_{k_1,k_2,l_1,l_2}^{k,l\,(+)} = \left\langle Q^+ \left(\varphi_{k_1}^{(\beta)}\xi_{l_1}, \varphi_{k_2}^{(\beta)}\xi_{l_2} \right), \varphi_k^{(\beta)}\xi_l \right\rangle_{L^2(\mathbb{R}^2;\beta)}$$

$$= \frac{1}{2\pi} \int_{\mathbb{R}^2} \int_{\mathbb{R}^2} \int_{\mathbb{S}^1} B(\|\boldsymbol{v}-\boldsymbol{v}_*\|,\cos\theta) \left(\varphi_{k_1}^{(\beta)}\xi_{l_1} \right)(\boldsymbol{v}') \left(\varphi_{k_2}^{(\beta)}\xi_{l_2} \right)(\boldsymbol{v}'_*)$$

$$\left(\mu^{1-2/\beta}\varphi_k^{(\beta)}\xi_{-l} \right)(\boldsymbol{v})\,\mathrm{d}\boldsymbol{\sigma}\,\mathrm{d}\boldsymbol{v}_*\,\mathrm{d}\boldsymbol{v}$$

$$= \frac{1}{2\pi} \int_{\mathbb{R}^2} \left(\varphi_{k_1}^{(\beta)}\xi_{l_1} \right)(\boldsymbol{v}) \int_{\mathbb{R}^2} \left(\varphi_{k_2}^{(\beta)}\xi_{l_2} \right)(\boldsymbol{v}_*)\mathscr{I}_{k,l}^+(\boldsymbol{v},\boldsymbol{v}_*)\,\mathrm{d}\boldsymbol{v}_*\,\mathrm{d}\boldsymbol{v}$$

with

$$\mathscr{I}_{k,l}^+(\boldsymbol{v},\boldsymbol{v}_*) = \int_{\mathbb{S}^1} B(\|\boldsymbol{v}-\boldsymbol{v}_*\|,\cos\theta) \left(\mu^{1-2/\beta}\varphi_k\xi_{-l} \right)(\boldsymbol{v}')\,\mathrm{d}\boldsymbol{\sigma}. \tag{4.2}$$

Here, we have made a change of variables $\boldsymbol{v},\boldsymbol{v}_* \longleftrightarrow \boldsymbol{v}',\boldsymbol{v}'_*$, revealing a striking similarity with the loss term. However, in this case we find the (k,l)-dependence in the inner integral, which makes the gain term somewhat more challenging, even for simple cases like the Maxwellian kernel.

In analyzing $\mathscr{I}^+$ it will be helpful to identify the points $\boldsymbol{v},\boldsymbol{v}_*$ in velocity space with complex numbers (Note, however, that while the integrals are complex-valued, they are not complex integrals.). In the following, let us also make the simplifying assumption of considering only constant $b(\cos\theta) \equiv 1$, known as the Variable Hard Spheres (VHS) assumption.

After making the substitution $\boldsymbol{v}' = e^{\mathrm{i}\arg(\boldsymbol{v}+\boldsymbol{v}_*)}\boldsymbol{w}'$, we find

$$\mathscr{I}_{k,l}^+(\boldsymbol{v},\boldsymbol{v}_*) = \|\boldsymbol{v}-\boldsymbol{v}_*\|^\lambda\,\xi_{-l}(\arg(\boldsymbol{v}+\boldsymbol{v}_*)) \int_{\mathbb{S}^1} \left(\mu^{1-2/\beta}\varphi_k^{(\beta)}\xi_l \right)(\boldsymbol{w}')\,\mathrm{d}\boldsymbol{\sigma}, \tag{4.3}$$

where now $\boldsymbol{w}'$ runs over a circle centered at $1/2\|\boldsymbol{v}+\boldsymbol{v}_*\|$ with radius $1/2\|\boldsymbol{v}-\boldsymbol{v}_*\|$ (see Figure 3). In particular, the integral in (4.3) is real, and depends only on the two real quantities $\|\boldsymbol{v}+\boldsymbol{v}_*\|$ and $\|\boldsymbol{v}-\boldsymbol{v}_*\|$ (and not on their arguments). Additionally, $\mathscr{I}^+$ depends on the argument of $\boldsymbol{v}+\boldsymbol{v}_*$, but this dependence is trivial and requires no quadrature to track. In out implementation we *precompute* $\mathscr{I}_{k,l}^+(\boldsymbol{v},\boldsymbol{v}_*)$ for relevant indices k,l and pairs of quadrature points on velocity space.

REMARK 4.4 Some of the listed advantages of the polar method over the Fourier discretization depend on the fact that the solution will converge to a function that lies in the solution space (in the conforming case), or if not, is isotropic and thus has a sparse representation. These conditions might fail to hold in the solution of a spatially *in*homogeneous Boltzmann equation, where the equilibrium solution might depend on the spatial variable $\boldsymbol{x}$ under certain source terms and boundary conditions. In this case, conformity can no longer be guaranteed at every point, nor can isotropy of the equilibrium be taken for granted (say, if the global momentum in the system is nonzero).

We have not performed experiments with the spatially inhomogeneous Boltzmann equation in this work. However, we have performed limited experiments in the homogeneous case where conformity and equilibrium isotropy are deliberately discarded. These results are discussed in Section 5.5. The results indicate that the method might still be viable in this case, and that adaptivity might still be useful, although the parameter choice $\beta = 2$ should be avoided.

5. Numerical results

Throughout this section, all quadrature in $\boldsymbol{v}$ has been performed using a polar tensor product quadrature rule with Gauss-Laguerre quadrature rules in the radial direction and the trapezoidal rule in the angular
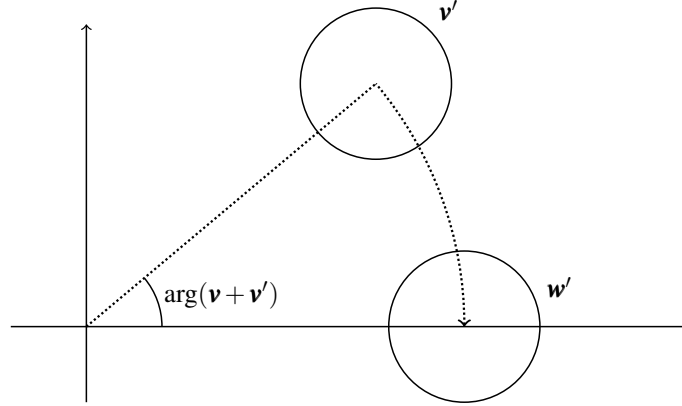
FIG. 3: Transforming the integral $\mathscr{I}^+$ from (4.2) to (4.3).

direction. For the computation of the collision tensor S, we used "overkill" 61-point quadrature in both directions (this includes 61-point trapezoidal quadrature for the inner integrals $\mathscr{I}^-$ and $\mathscr{I}^+$). Thus, we expect the impact of quadrature error to be negligible. For the evaluation of the initial condition and errors, we used the same quadrature rule.

Timestepping was performed using an explicit fourth-order Runge-Kutta method with a timestep of 10^{-2} for $\beta = 1$ and $5 \cdot 10^{-3}$ for $\beta = 2$, to compensate for the fact that after rescaling time runs twice as quickly in the latter case. Stiffness does not appear to be a problem.

5.1 *Validation for BKW solution*

The BKW solution Tourenne (1983); Ernst (1984) is the only known non-stationary analytic solution to (1.1). It takes the form

$$g(t,v) = (2\pi s)^{-d/2} \exp\left(-\frac{\|\mathbf{v}\|^2}{2s}\right) \left(1 - \frac{1-s}{2s}\left(d - \frac{\|\mathbf{v}\|^2}{s}\right)\right) \tag{5.1}$$

where

$$s = s(t) = 1 - e^{-\lambda(t+t_0)},$$

and $B = $ const. (also called the *Maxwellian* kernel). Here, λ is a parameter given in terms of B, and for $d = 2$ we find $B = \frac{1}{2\pi}$ and $\lambda = \frac{1}{8}$. Finally, t_0 is any reasonable starting time so that $g(t,v) \geqslant 0$ everywhere. We will use a t_0 determined by $s(0) = \frac{1}{2}$, which gives the initial distribution

$$g_0(\mathbf{v}) = \frac{1}{\pi}\|\mathbf{v}\|^2 e^{-\|\mathbf{v}\|^2}.$$

With g so defined, write

$$f(t,\mathbf{v}) = 2\pi g(2\pi t, \mathbf{v}). \tag{5.2}$$

Then f is a 2-conforming solution to (1.1), and $f(t/2, \sqrt{2}\mathbf{v})$ is the corresponding 1-conforming solution.

The L^2-errors for this test are shown, depending on t, K and β, in Figures 4 on the following page and 5 on page 21. One can observe exponential convergence to zero both in K and t, as expected. No dependence on L is shown, since g is isotropic for all times.

We observe that the error decays exponentially to a threshold level for all K. This threshold is mostly due to quadrature error, and not timestepping. The $\beta = 2$ method is better for solutions far removed from equilibrium, but $\beta = 1$ eventually achieves better accuracy.
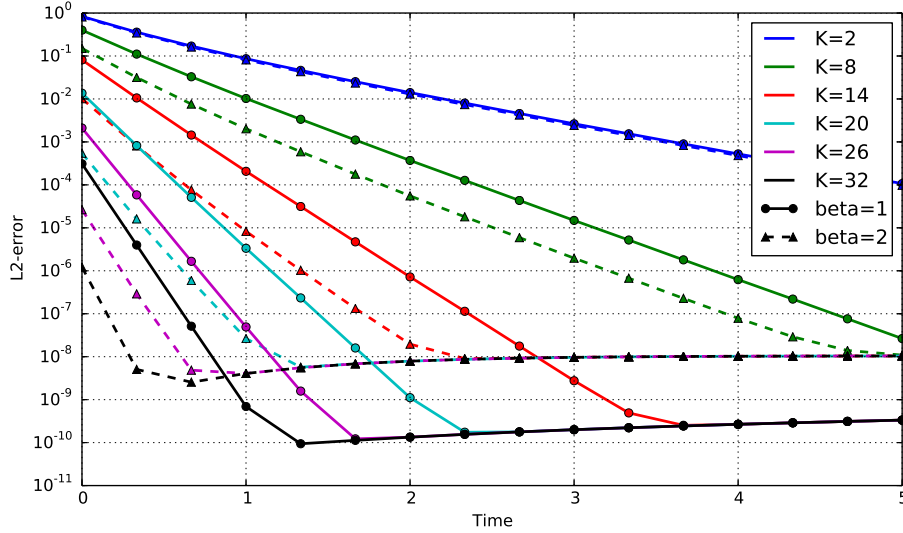
FIG. 4: L^2-error for the BKW solution as a function of time for different radial resolutions K and values of β, see Section 5.1 on the previous page for details.

5.2   Crossed streams

Given constants $R, S > 0$, a 2-conforming crossed streams initial condition can be constructed as follows:

$$\eta(c, v, w) = \exp\left[-g(S(v-c)^2 + (w-c)^2)\right]$$
$$f_0(\boldsymbol{v}) = \alpha\left(\eta(c, v_x, v_y) + \eta(-c, v_y, v_x)\right)$$

with

$$\delta = 4R^2 + \frac{1}{S} + 1, \qquad \alpha = \frac{\delta}{4}\sqrt{S}, \qquad g = \frac{\delta}{4}, \qquad c = \frac{R}{\sqrt{g}}.$$

Here, R regulates the relative velocity between the two streams, and S the relative spread of the two streams in each direction (parallel and perpendicular to the momentum).

Figure 6 on page 22 shows some samples of approximate solutions to this initial condition with $S = 3, R = 1$, with a relatively large number of degrees of freedom.

Figure 7 on page 23 shows the error in observables as a function of time for both values of β. As expected, $\beta = 1$ is considerably more accurate than $\beta = 2$. The experiment also shows a slight unexpected worsening of the energy and momentum for $\beta = 1$, which should be constant. This can likely be attributed to quadrature error.
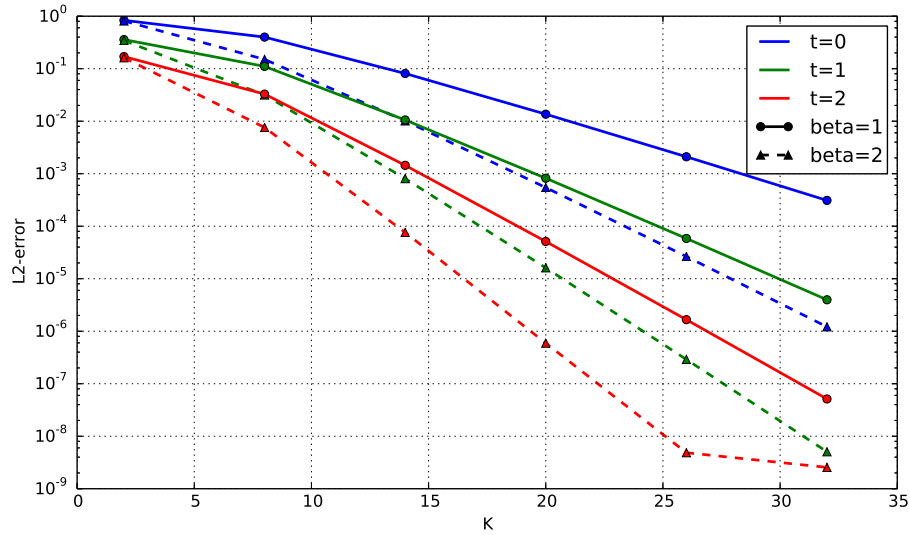
FIG. 5: L^2-error for the BKW solution as a function of the number K of radial basis function for different times t and values of β, see Section 5.1 on page 19 for details.

Figure 10 on page 25 shows the entropy of the numerical solution as a function of time for $K = 44$, $L = 26$. For the concept of entropy refer to (Cercignani, 2002, Section 8).

In Figure 8 on page 24, the evolution of the spectral coefficients are shown. One may observe that coefficients approach zero in columns (with constant l), which validates the adaptive strategy from Remark 4.1.

Finally, Figure 9 on page 25 shows the time-dependent power contribution for some values of k, for $\beta = 2$. The power contribution of level k is defined as the time-dependent quantity

$$\sum_l |F_{k,l}(t)|^2.$$

(a) $\beta = 1$

(b) $\beta = 2$
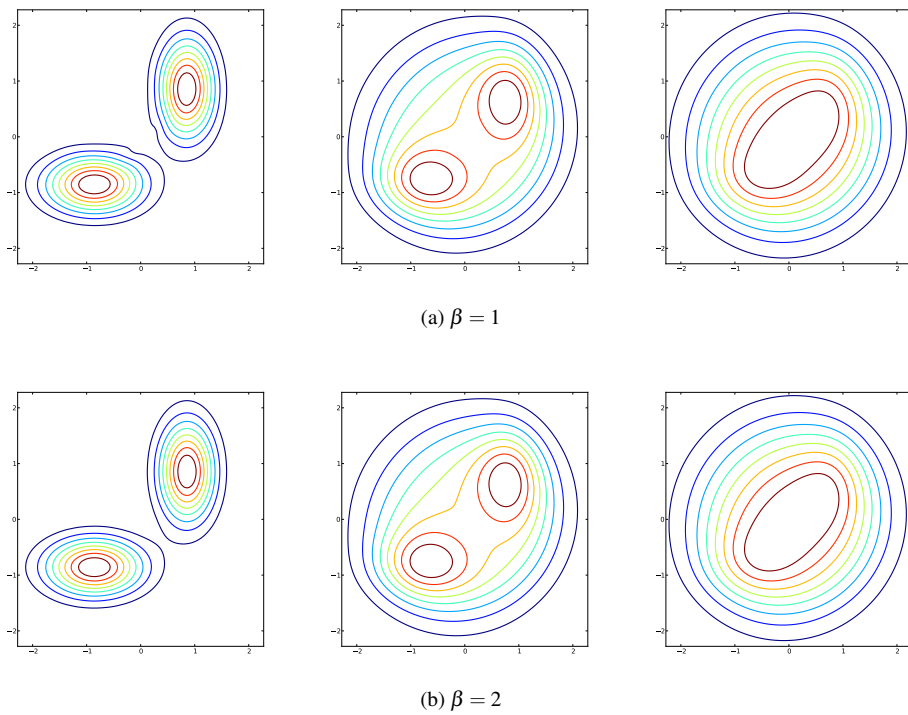
FIG. 6: Solutions to the crossed streams experiment with $K = 44$, $L = 26$. The times shown are, from left to right, $t = 0, 0.5, 0.75$. See Section 5.2 on page 20 for details.
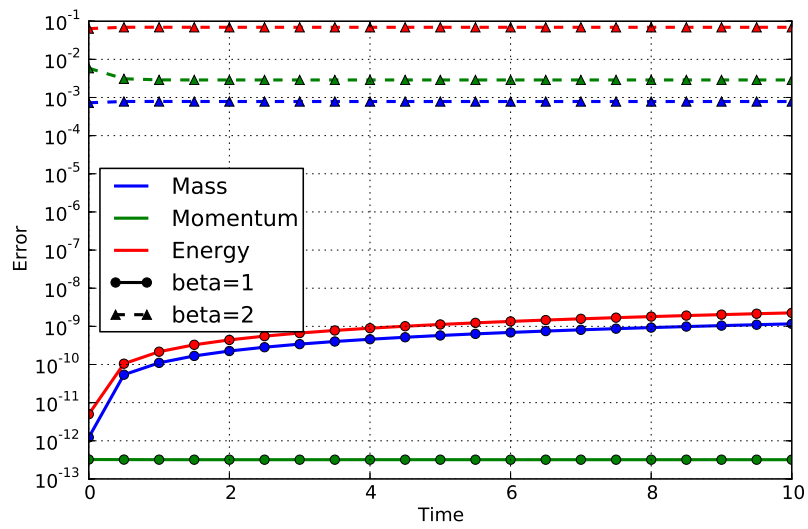
FIG. 7: Error in observables at different times for the crossed streams experiment. The progressive worsening of mass and energy for $\beta = 1$ is attributed to quadrature error. See Section 5.2 on page 20 for details.
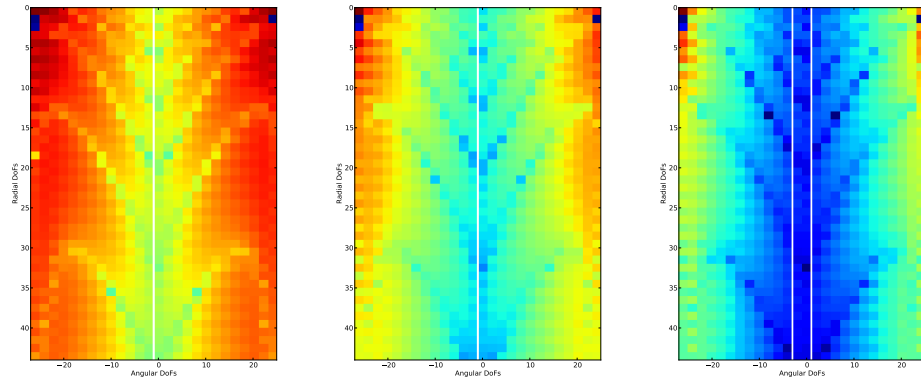
(a) $\beta = 1$
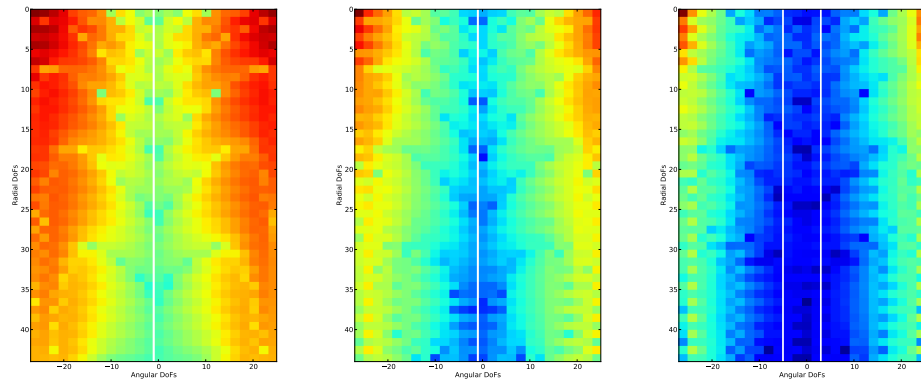
(b) $\beta = 2$

FIG. 8: Spectral magnitudes for the crossed streams experiment. The times shown are, from left to right, $t = 0, 2.1, 4.2$. The adaptive restriction of the function space is indicated with white lines, using a threshold value of 10^{-10}. See Section 5.2 on page 20 for details.
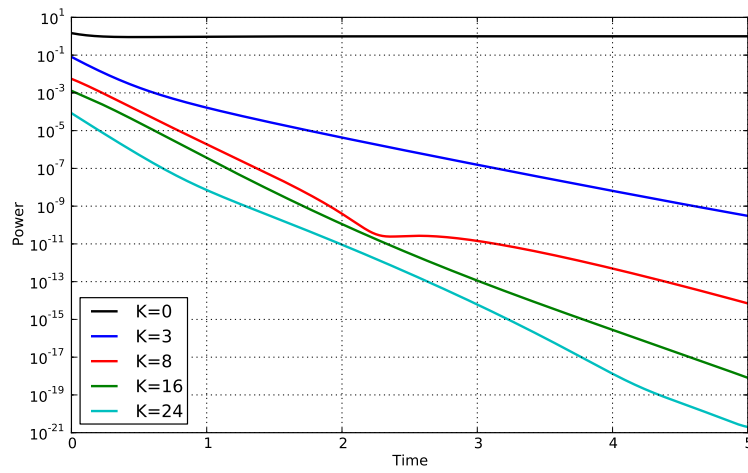
FIG. 9: Power contribution for some values of *k* for the crossed streams experiment. See Section 5.2 on page 20 for details.
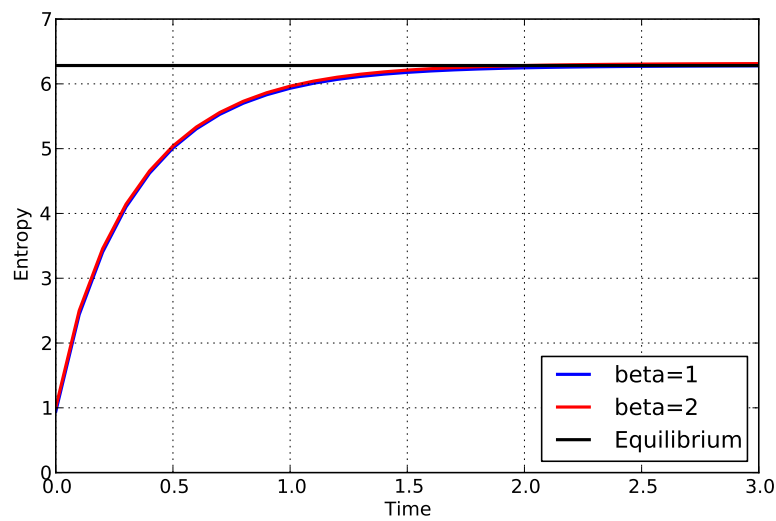
FIG. 10: Entropy as a function of time for the crossed streams experiment. See Section 5.2 on page 20 for details.

5.3 *Adaptivity*

In Figure 11 we show the time-dependence of the computational effort per timestep (a pseudo-quantity of L^2), under the strategy detailed in Remark 4.1. The results shown are for three different experiments, one of which (blue) is the crossed streams of the previous section. In this particular case we used a threshold value of 10^{-10}, which can be considered very strict.

We observe a strong downward tendency in all cases. One achieves better adaptivity for $\beta = 2$ than $\beta = 1$, but this difference does not appear to be significant compared to the dependence on the actual initial data.
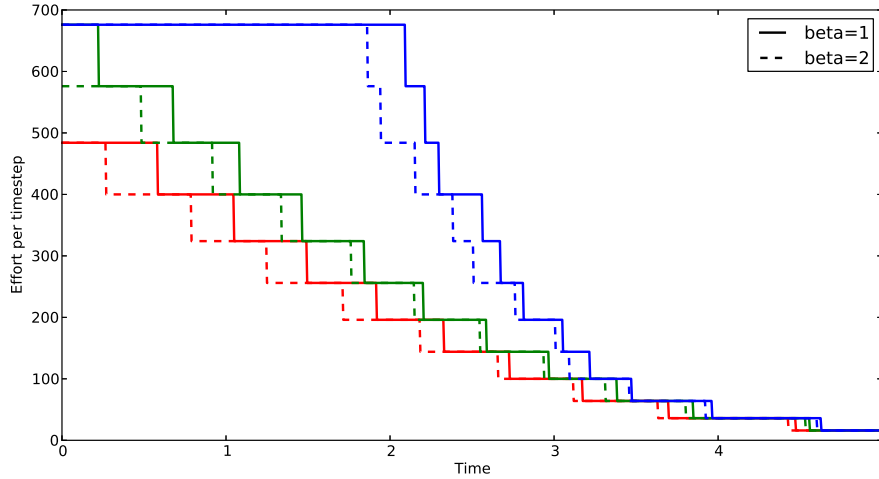
FIG. 11: Time-dependence of computational effort per timestep ($\propto L^2$) for three different experiments (red is the crossed streams solution of Section 5.2 on page 20, blue is the initial condition $\frac{5}{4}\exp(-\frac{5}{16}(4v_x^2 + v_y^2))$, and green is the initial condition $\alpha\left[\exp(-\alpha|\boldsymbol{v} - \boldsymbol{\eta}|^2) + \frac{1}{2}\exp(-\frac{\alpha}{2}|\boldsymbol{v} + \boldsymbol{\eta}|^2)\right]$ where $S = 1.8$, $\alpha = \frac{1}{4}(3 + 2S^2)$ and $\eta = S\alpha^{-1/2}$. (The latter two are given in their $\beta = 2$-conforming cases.) See Section 5.3 for details.

5.4 *Collision tensor compressibility*

Figure 12 on the facing page shows the magnitude of the nonzero collision tensor entries for $K = 44$ and $L = 26$ (giving about 20 million nonzero entries) for both $\beta = 1$ and $\beta = 2$. One might hope that a sufficiently rapid decay in these entries can yield some compressibility of the tensor, but this appears not to be the case, particularly not for $\beta = 2$.

5.5 *Non-conforming solutions*

In light of the discussion in Remark 4.4, we study here the performance of the Polar method for a non-conforming solution which has off-center momentum. The equilibrium solution is thus neither in the
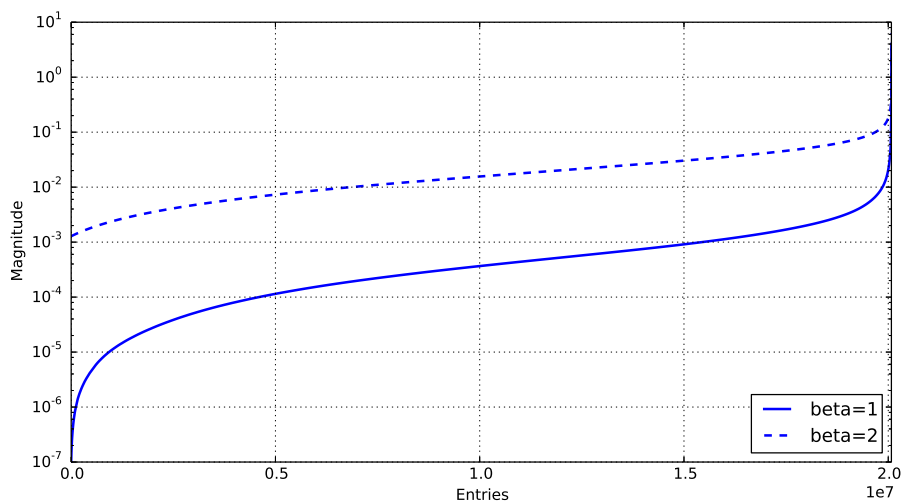
FIG. 12: Magnitudes of the roughly 20 million nonzero collision tensor entries for $K = 44$ and $L = 26$. See Section 5.4 on the facing page for details.

solution space, nor is it isotropic. Specifically, we have used the initial condition

$$f_0(\boldsymbol{v}) = \exp\left[-5\|\boldsymbol{v}\|^2\right] + \exp\left[-5(v_x - 1)^2 - 12v_y^2\right],$$

which represents a stream of gas colliding with gas at equilibrium.

Figure 13 on the next page shows contour plots of the solutions to this experiment at various times for both $\beta = 1$ and $\beta = 2$.

Figure 15 on page 30 shows the evolution of the spectral coefficients, and should be compared to Figure 8 on page 24. The general pattern of coefficient decay appears to be maintained, although it is considerably slower, and will not go as far.

Finally, Figure 14 on page 29 shows the time-dependent power contribution for some values of k, for $\beta = 2$, and should be compared to Figure 9 on page 25. The power content of the higher levels can be seen to deteriorate for longer times in the $\beta = 2$ case, which might be related to the poor stability of the method and the lack of symmetry of the solution. The $\beta = 1$ solutions suffer no such effects.

6. Comparison with Fourier discretization

We offer here some concluding remarks on the viability of the two methods presented.

With N^2 degrees of freedom, the Fourier discretization can perform a timestep in $\mathscr{O}(N^4)$ time, and with KL degrees of freedom, the Polar discretization uses $\mathscr{O}(K^3L^2)$ time per timestep. In addition to this, the convergence in radial direction is only $\mathscr{O}(\mathrm{e}^{-\sqrt{K}})$ compared to $\mathscr{O}(\mathrm{e}^{-N})$ in all directions for the Fourier discretization, assuming an analytic solution. Both methods require a one-time setup where the discrete collision operator is computed, but this step depends only on the kernel.
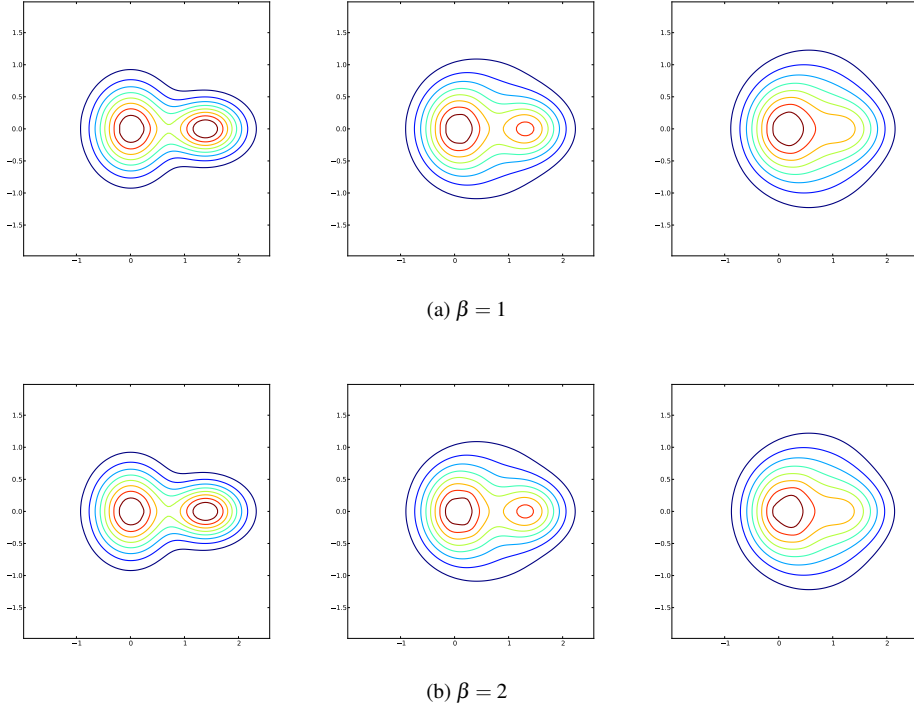
(a) $\beta = 1$

(b) $\beta = 2$

FIG. 13: Nonconforming experiment with $K = 44$, $L = 26$. The times shown are, from left to right, $t = 0, 0.5, 1.0$. See Section 5.5 on page 26 for details.

With this in mind, it seems unlikely that the Polar discretization can outperform the Fourier method. It can be argued that the Polar method will yield more physical solutions (especially for $\beta = 1$), as it is both fully conservative and devoid of aliasing effects. The Polar method also performs exceptionally well with near-equilibrium solutions, while the Fourier method has constant performance across the board (or possibly, as the case may be for the hyperbolic cross method, it performs well for some solutions that are far removed from equilibrium).

It has proven challenging to directly compare the error performance of the two methods in a realistic experiment. Since the only known exact solution to (1.1) is the isotropic BKW solution (which gives the Polar method an unfair advantage), we have to resort to reference solutions computed with very high accuracy. For this, we have again used the crossed streams solution of Section 5.2 on page 20.

Reference solutions were computed using the full Fourier method (with $100 \times 100 = 10^4$ degrees of freedom), and with the Polar method (with $44 \times 26 = 1144$ degrees of freedom). The comparison solutions were computed for the Fourier method on $N \times N$-grids for $N = 8, 10, 12, 14$, and for the Polar method on $N \times N/2$-grids for $N = 12, 16, 20$. These numbers give comparable total numbers of degrees of freedom ($[64, 196]$ for Fourier and $[72, 200]$ for Polar).

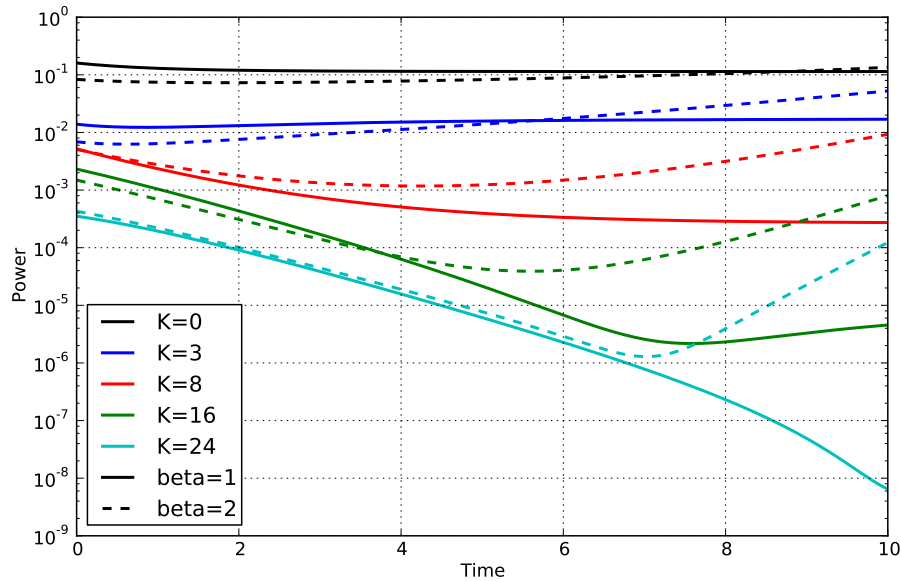The results of this experiment can be seen in Figure 16. The cross-method errors are all dominated

FIG. 14: Power contribution for some values of *k* for the nonconforming experiment. See Section 5.5 on page 26 for details.

by the difference between the two reference solutions, and consistently level off at about 10^{-2} (see Figure 17). This disagreement between the methods can presumably be explained by either

(i) dissipative effects from explicit timestepping, or

(ii) aliasing error introduced in the Fourier method.

As an additional experiment, we have performed the same analysis on the nonconforming solution of Section 5.5, while all other values remain the same (grid sizes, etc.), except we have used $\beta = 1$, since from the observations made in Figure 9 on page 25, the $\beta = 2$ method is may not be reliable for nonconforming (or at least, asymmetrical) solutions. The relevant data can be seen in Figure 18 on page 33.

Here, the two methods perform comparably well, and the error is *not* dominated by the difference between the reference solutions, but rather by the actual discretization error.

To be able to evaluate more accurately the quality of the two reference solutions we have performed the same test on the BKW solution, which has a known nontrivial analytic solution. The results are shown in Figure 19 on page 34, which shows the time-dependent errors for the polar method (with 44 radial basis functions), and for three different full-grid Fourier methods with 80×80 degrees of freedom, differing only in the parameter L, to attempt to control the aliasing error. The errors were computed only on the square $[-\pi/2, \pi/2]^2$, which is the domain of the smallest Fourier experiment. We observe that the polar method produces significantly better solutions.
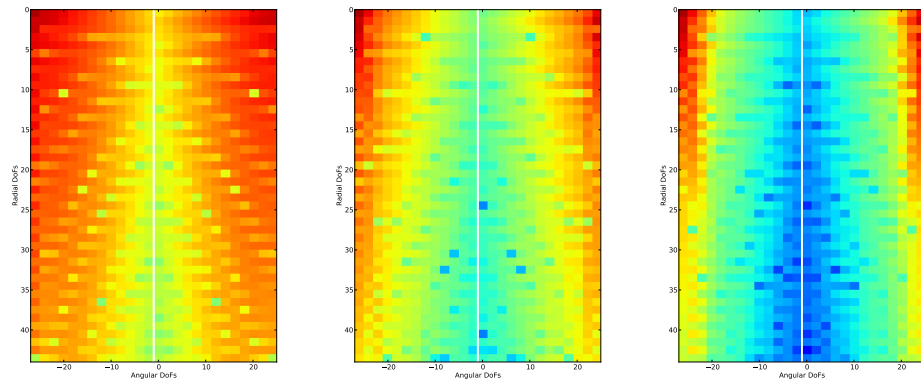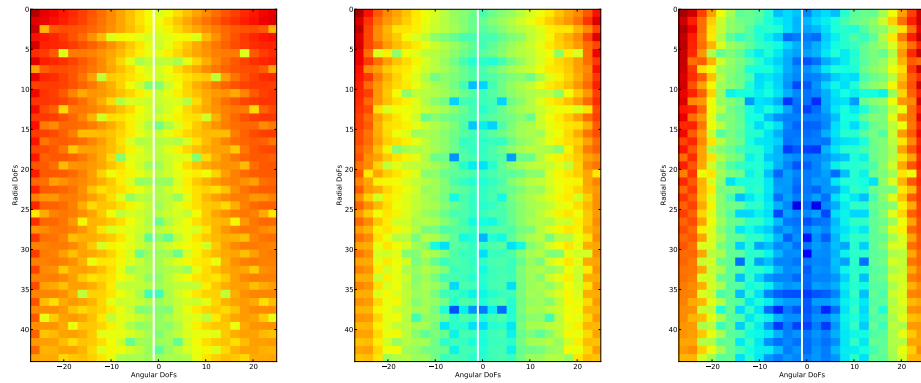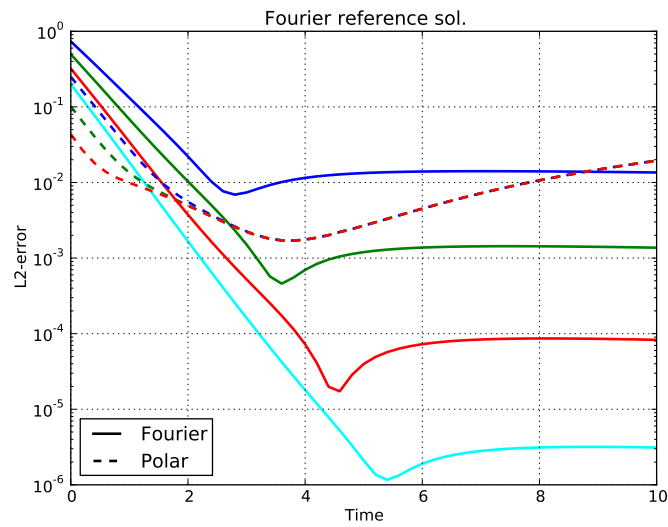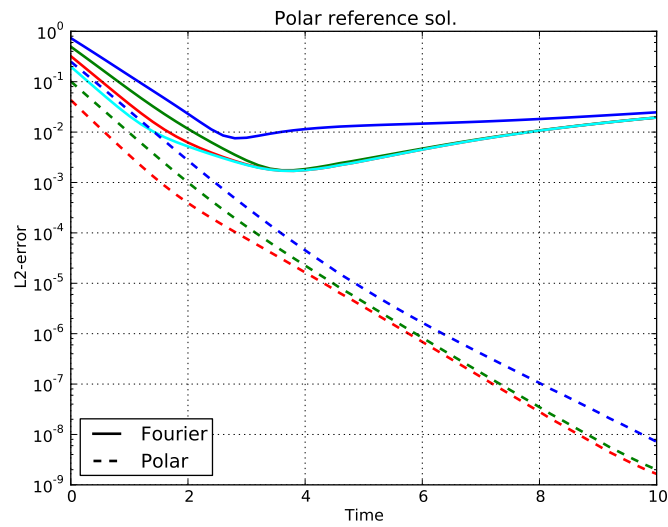
(a) $\beta = 1$

(b) $\beta = 2$

FIG. 15: Spectral magnitudes for the nonconforming experiment. The times shown are, from left to right, $t = 0, 5, 10$. No adaptivity was achieved here with a strict threshold value of 10^{-10}. Compare to Figure 8. See Section 5.5 on page 26 for details.

(a) Reference solution computed with the Fourier method.

(b) Reference solution computed with the Polar method.

FIG. 16: Comparison using reference solutions computed with the two different methods for the crossed streams experiment. Note the *y*-axis scales. See Section 6 on page 27 for details.
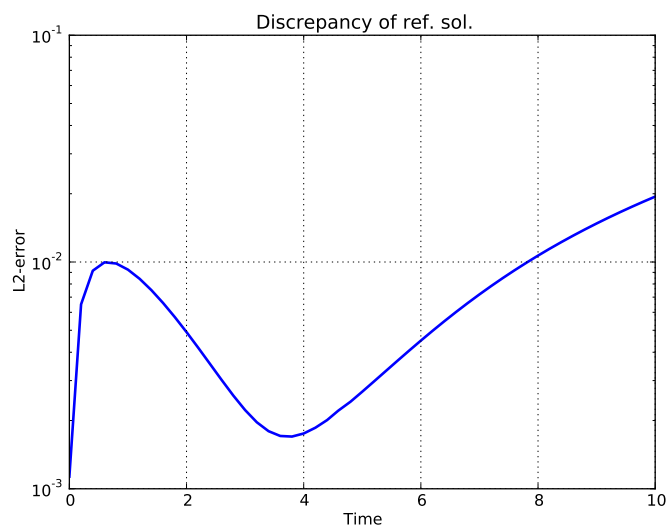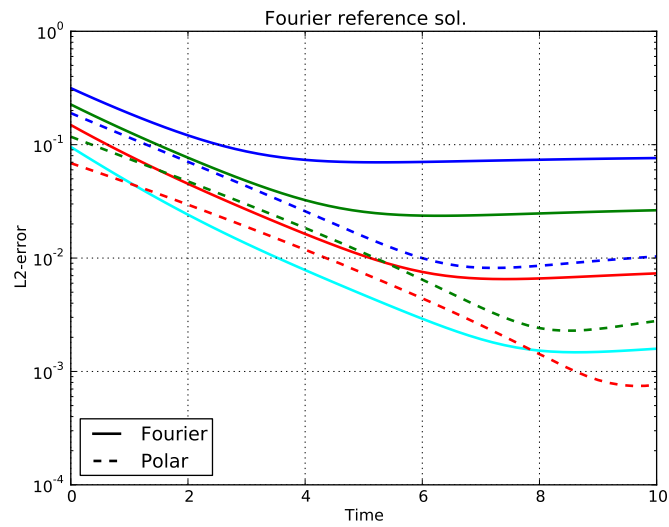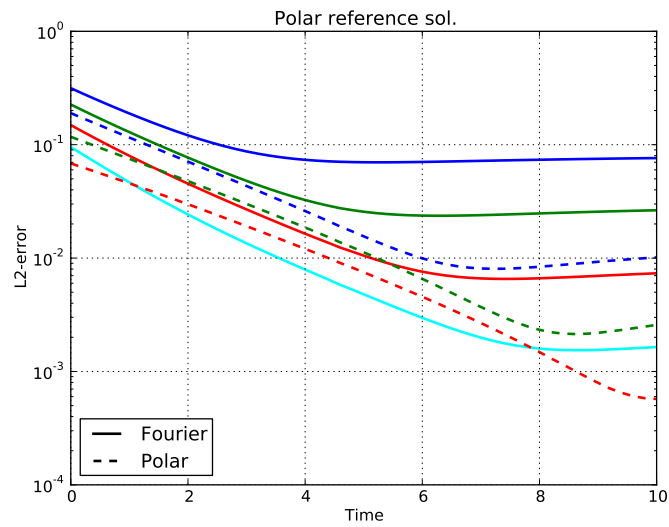
FIG. 17: The discrepancy between the two reference solutions from the crossed streams experiment of Figure 16, measured in the L^2-norm. See Section 6 on page 27 for details.

(a) Reference solution computed with the Fourier method.

(b) Reference solution computed with the Polar method.

FIG. 18: Comparison using reference solutions computed with the Fourier method (top) and Polar method (middle) for the nonconforming experiment. See Section 6 on page 27 for details.
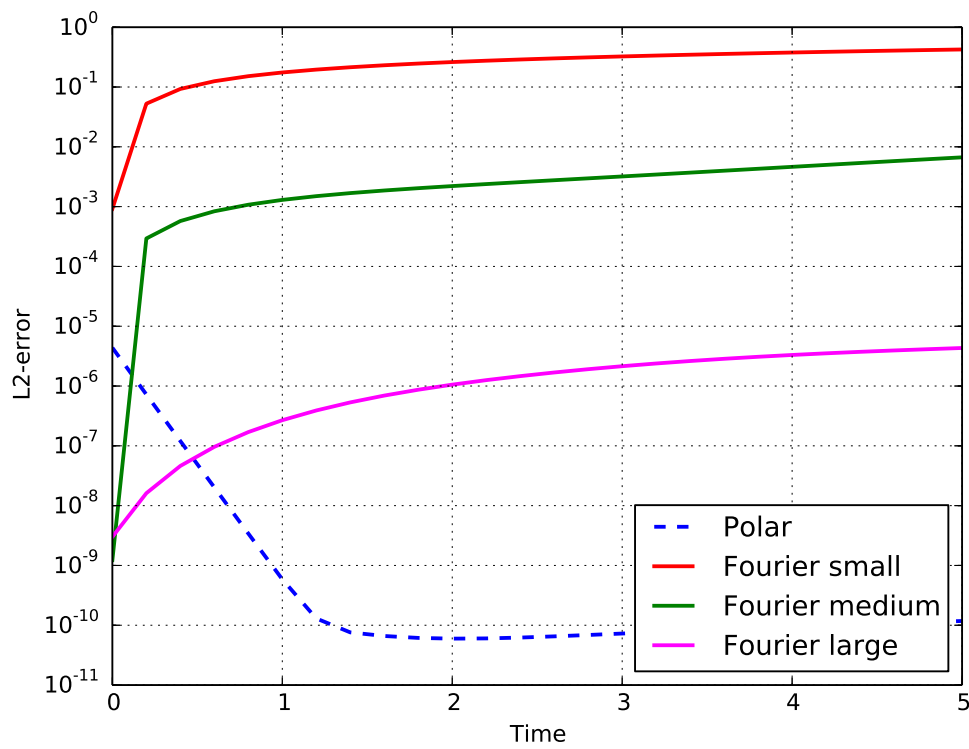
FIG. 19: Comparison between reference solutions for the BKW solution, defined as $g(t/2, \sqrt{2}\boldsymbol{v})$ for g from (5.2). We used $L = \pi/2, \pi, 3\pi/2$ for the three different Fourier solutions (small, medium and large, respectively) in order to control aliasing errors. The Fourier solutions were produced with 80×80 degrees of freedom, and the polar solution with 44 radial degrees of freedom. See Section 6 on page 27 for details.

References

BOBYLEV, A. V. (1988) The theory of the nonlinear spatially uniform Boltzmann equation for Maxwell molecules. *Soviet Sci. Rev. Sect. C Math. Phys. Rev.*, **7**, 110–233.

BOBYLEV, A. V. & RJASANOW, S. (1997) Difference scheme for the Boltzmann equation based on the fast Fourier transform. *European J. Mech. B Fluids*, **16**, 293–306.

BOBYLEV, A. V. & RJASANOW, S. (1999) Fast deterministic method of solving the Boltzmann equation for hard spheres. *Eur. J. Mech. B Fluids*, **18**, 869–887.

BOBYLEV, A. V. & RJASANOW, S. (2000) Numerical solution of the Boltzmann equation using a fully conservative difference scheme based on the fast Fourier transform. *Transport Theory Statist. Phys.*, **29**, 289–310.

CERCIGNANI, C. (2002) The Boltzmann equation and fluid dynamics. *Handbook of Mathematical Fluid Mechanics*, vol. 1. Amsterdam: Elsevier, pp. 1–69.

ENDER, A. Y. & ENDER, I. A. (1994) Moment methods for the isotropic Boltzmann equation. *Journal of Technical Physics*, **64**, 38–53. In russian.

ENDER, A. Y. & ENDER, I. A. (1999) Polynomial expansions for the isotropic Boltzmann equation and invariance of the collision integral with respect to the choice of basis functions. *Physics of Fluids*, **11**, 2720–2730.

ERNST, M. H. (1984) Exact solutions of the nonlinear Boltzmann equation. *Journal of Statistical Physics*, **34**, 1001–1017.

FILBET, F., MOUHOT, C. & PARESCHI, L. (2006) Solving the Boltzmann equation in $N \log_2 N$. *SIAM J. Sci. Comput.*, **28**, 1029–1053.

FILBET, F. & MOUHOT, C. (2011) Analysis of spectral methods for the homogeneous Boltzmann equation. *Transactions of the American Mathematical Society*, **363**, 1947–1980.

FONN, E., GROHS, P. & HIPTMAIR, R. (2012) Hyperbolic cross approximation for the spatially homogeneous boltzmann equation. *Report* 2012-28. Zürich, Switzerland: SAM, ETH Zürich. Submitted to IMA J. Numer. Anal.

GAMBA, I. M. & THARKABHUSHANAM, S. H. (2009) Spectral-Lagrangian methods for collisional models of non-equilibrium statistical states. *Journal of Computational Physics*, **228**, 2012 – 2036.

GAMBA, I. M. & THARKABHUSHANAM, S. H. (2010) Shock and boundary structure formation by spectral-Lagrangian methods for the inhomogeneous Boltzmann transport equation. *J. Comput. Math.*, **28**, 430–460.

GAVRILYUK, I. & KHOROMSKIJ, B. (2011) Quantized-TT-Cayley transform for computing the dynamics and the spectrum of high-dimensional Hamiltonians. *Comput. Methods Appl. Math.*, **11**, 273–290.

IBRAGIMOV, I. & RJASANOW, S. (2002) Numerical solution of the Boltzmann equation on the uniform grid. *Computing*, **69**, 163–186.

IVANIC, J. & RUEDENBERG, K. (1996) Rotation matrices for real spherical harmonics. Direct determination by recursion. *The Journal of Physical Chemistry*, **100**, 6342–6347.

KIRSCH, R. & RJASANOW, S. (2007) A weak formulation of the Boltzmann equation based on the Fourier transform. *J. Stat. Phys.*, **129**, 483–492.

KITZLER, G. & SCHÖBERL, J. (2013) Efficient spectral methods for the spatially homogenous Boltzmann equation. available as ASC Report No. 13/2013, TU Vienna.

LESSIG, C., DE WITT, T. & FIUME, E. (2012) Efficient and accurate rotation of finite spherical harmonics expansions. *Journal of Computational Physics*, **231**, 243 – 250.

MOUHOT, C. & PARESCHI, L. (2006) Fast algorithms for computing the Boltzmann collision operator. *Math. Comput.*, **75**, 1833–1852.

PARESCHI, L., TOSCANI, G. & VILLANI, C. (2003) Spectral methods for the non cut-off Boltzmann equation and numerical grazing collision limit. *Numerische Mathematik*, **93**, 527–548.

PARESCHI, L. & PERTHAME, B. (1996) A Fourier spectral method for homogeneous Boltzmann equations. *Transport Theory Stat. Phys.*, **25**, 369–383.

PARESCHI, L. & RUSSO, G. (2000) Numerical solution of the Boltzmann equation I: spectrally accurate approximation of the collision operator. *SIAM J. Numer. Anal.*, **37**, 1217–1245.

RJASANOW, S. & WAGNER, W. (2005) *Stochastic numerics for the Boltzmann equation*. Springer Series in Computational Mathematics, vol. 37. Berlin: Springer-Verlag, pp. xiv+256.

SZSZ, O. & YEARDLEY, N. (1958) The representation of an analytic function by general Laguerre series. *Pacific Journal of Mathematics*, **8**, 621–633.

TOURENNE, C. J. (1983) The entropy of the BKW solution. *Journal of Statistical Physics*, **32**, 71–80.

VILLANI, C. (2002) A review of mathematical topics in collisional kinetic theory. *Handbook of Mathematical Fluid Mechanics*, vol. 1. Amsterdam: Elsevier, pp. 71–305.

WIGNER, E. (1944) *Gruppentheorie und ihre Anwendung auf die Quantenmechanik der Atomspektren*. J. W. Edwards, Ann Arbor, Michigan, pp. viii+332.

Recent Research Reports

Nr.	Authors/Title

2014-03   K. Grella
           Sparse tensor phase space Galerkin approximation for radiative transport

2014-04   A. Hiltebrand and S. Mishra
           Efficient preconditioners for a shock capturing space-time discontinuous Galerkin
           method for systems of conservation laws

2014-05   X. Claeys and R. Hiptmair and C. Jerez-Hanckes and S. Pintarelli
           Novel Multi-Trace Boundary Integral Equations for Transmission Boundary Value
           Problems

2014-06   X. Claeys and R. Hiptmair
           Integral Equations for Acoustic Scattering by Partially Impenetrable Composite
           Objects

2014-07   P. Grohs and S. Keiper and G. Kutyniok and M. Schaefer
           Cartoon Approximation with α -Curvelets

2014-08   P. Grohs and M. Sprecher and T. Yu
           Scattered Manifold-Valued Data Approximation

2014-09   P. Grohs and U. Wiesmann and Z. Kereta
           A Shearlet-Based Fast Thresholded Landweber

Algorithm for Deconvolution

2014-10   P. Grohs and S. Vigogna
           Intrinsic Localization of Anisotropic Frames II: α-Molecules

2014-11   S. Etter and P. Grohs and A. Obermeier
           FFRT - A Fast Finite Ridgelet Transform for Radiative Transport